

University of Nevada, Reno

Climate Impacts on Streamflow Dynamics of Mammoth Creek and
the Upper Owens River, California

A thesis submitted in partial fulfillment
of the requirements for the degree of Master of Science in Hydrology

by

Susan Burak

Dr. Justin Huntington, Thesis Advisor

August, 2015



THE GRADUATE SCHOOL

We recommend that the thesis
prepared under our supervision by

SUSAN BURAK

Entitled

**Climate Impacts On Streamflow Dynamics Of Mammoth Creek And The Upper
Owens River, California**

be accepted in partial fulfillment of the
requirements for the degree of

MASTER OF SCIENCE

Justin Huntington, Ph. D., Advisor

Scott Tyler, Ph. D., Committee Member

John Naliboff, Ph. D., Committee Member

Jim Thomas, Ph.D., Graduate School Representative

David W. Zeh, Ph. D., Dean, Graduate School

August, 2015

Abstract

Mammoth Creek and the Upper Owens River, located in the eastern Sierra Nevada, are the primary headwater supply for Mono County and the City of Los Angeles. Population and economic growth continue to increase pressures on water supplies in the Town of Mammoth Lakes and Los Angeles, therefore a more thorough understanding on the physical processes and empirical relationships between climate and streamflow in these headwaters is warranted. Climate in the study area is characterized by large-scale features of general circulation and orography, resulting in high spatial and temporal variability. Snowmelt provides for groundwater recharge and streamflow throughout the spring, early summer, and late season low flow periods.

This thesis examines how lags between climate and streamflow are related to headwater catchment geology and hydrogeology. Empirical relationships between climate and streamflow are evaluated for Mammoth Creek and the Upper Owens River with the Standardized Precipitation Evapotranspiration Index (SPEI) at 12, 15, 24, 36, and 48-month timescales, and standardized streamflows. The SPEI provides a useful basis for interpreting hydrologic regimes in this area because the impacts of climate variability on streamflow occur at a range of time scales and are largely a function of the hydrogeology.

Results indicate that SPEI is well correlated at short timescales of 12 to 15 months in granitic and alluvial watersheds of the Mammoth Creek, whereas the SPEI is well correlated at longer time scales of 48 months in volcanic watersheds of the upper Owens River. These results paired with the hydrogeologic setting of the watersheds suggest that

the relatively impermeable granitic mountain block watershed of Mammoth Creek limits deep subsurface flow and groundwater storage, while more permeable volcanic rocks of the upper Owens River allow for deep groundwater recharge, storage, and sustained baseflow. Silicate weathering of volcanic rocks, age dating of water and naturally occurring isotopes of water support the timescales identified by the SPEI. Findings from this study highlight and reaffirm the lesser-known multi-time scale linkages between climate variability, hydrogeology, and hydrologic regimes of Mammoth Creek, Hot Creek and the upper Owens River using drought and streamflow indices.

Acknowledgements

Many people supported and encouraged me during this lengthy thesis process; a few notable mentors stand out.

Chris Farrar, USGS hydrologist, willingly shared his extensive knowledge of the geology and hydrology of the Long Valley caldera.

Tim Alpers, whose long family history living and raising trophy trout in the spring waters along the upper Owens River imbued him with a love of the spring resources of the upper Owens River.

Dan McEvoy, for his patient explanations of the Standardized Precipitation Evapotranspiration Index (SPEI) and for running Matlab code to produce SPEI data used in this work.

Sincere thanks goes to Greg Reis, Mono Lake Committee, Charlotte Rodriguez, Department of Water and Power, Irene Yamashita and Clay Murray of the Mammoth Community Water District for providing streamflow data.

I thank Dr. John Naliboff, Dr. Laura Waters and Benjamin Hatchett for their thoughtful reviews.

Finally, I would have never been able to finish my thesis without the guidance of Dr. Justin Huntington, who brought order to chaos.

TABLE OF CONTENTS

Abstract page	i
Acknowledgements	iii
Table of Contents	iv
List of Tables	vi
List of Figures	vii
I. INTRODUCTION	1
2. Environmental Setting	3
2.1 Regional Setting	3
2.2 Previous Research on the Hydrology of the Long Valley Caldera	5
2.3 Local Setting	7
2.4. Climate	11
3. Methods	12
3.1 Climate data	12
3.2 Hydrologic data	13
3.3. Calculations of SPEI	13
4. Results	15
4.1 Geologic and Hydrologic Relationships	15
4.2 SPEI	16
4.3 SPEI and Standardized Streamflow	19
4.4 Monthly Correlations between SPEI and Streamflow	19

5. Discussion	19
6. Conclusions and Future Work	22
Literature	28
Appendices	
Appendix A. Water chemistry, Upper Owens River watershed	35
Appendix A. Water chemistry discussion	37
Appendix B: SPEI Formulation	38

List of Tables

Table 1	General characteristics of the study watersheds.	47
Table 2	Precipitation stations.	47
Table	List of precipitation stations described in the text.	48
Table 4	SPEI drought classification	52

List of Figures

<u>Figure</u>		<u>Page</u>
Figure 1	Location map of study area.	42
Figure 2	Shaded relief map, Long Valley caldera.	43
Figure 3	Geological map of the Long Valley caldera.	44
Figure 4	Watershed areas and streamflow gages.	45
Figure 5	Mammoth Creek watershed.	46
Figure 6	Snowmelt discharge hydrology, upper Owens River, Mammoth Creek and Hot Creek.	48
Figure 7	Departure from mean annual streamflow, upper Owens River at East Portal.	49
Figure 8	Departure from mean annual streamflow, Mammoth Creek at DWP 395 gage.	49
Figure 9	Departure from mean annual streamflow, Hot Creek at Hot Creek Flume.	50
Figure 10	Average of the annual hydrograph for the wettest and driest 5 years of record of upper Owens River flows.	50
Figure 11	Average of the annual hydrograph for the wettest and driest 5 years of record at Mammoth Creek.	51
Figure 12	Average of the annual hydrograph for the wettest and driest 5 years of record at the Hot Creek Flume.	51
Figure 13	Historical time series of SPEI for the upper Owens River watershed at the 12, 24, 36 and 48-month time scales.	53
Figure 14	Historical time series of SPEI for the Mammoth Basin watershed at the 12, 24, 36 and 48-month time scales.	54
Figure 15	Continuous correlations between PRISM-based SPEI and standardized streamflow, Mammoth Creek, Hot Creek and the upper Owens River watersheds.	55

Figure 16	Temporal variability of the SPEI and standardized streamflow at the 15, 24 and 48- month scale, upper Owens River, East Portal.	56
Figure 17	Temporal variability of the SPEI and standardized Streamflow at the 15, 24, and 48-month time scale, Mammoth Creek at the DWP 395 gage.	57
Figure 18	Temporal variability of the SPEI and standardized streamflow at the 15, 24, and 48-month time scale, Hot Creek at the Hot Creek Flume.	58
Figure 19	Monthly correlations between SPEI and standardized streamflow and SPEI, upper Owens River at East Portal.	59
Figure 20	Monthly correlations between SPEI and standardized streamflow, Hot Creek at the Hot Creek Flume.	59
Figure 21	Monthly correlations between SPEI and standardized streamflow, Mammoth Creek at the DWP 395 gage.	60

1. Introduction

In the Eastern Sierra Nevada mountain range of California, snow comprises about 85 percent of annual precipitation, and snowmelt runoff provides about 50 percent of the water needs of the City of Los Angeles (MCWD 2010; Mono County, 2007). Seasonal snowpacks store water during winter for later release during spring snowmelt. Variability in California's annual precipitation presents significant challenges to water supply forecasts, particularly in areas of complex terrain such as Mammoth Creek and the upper Owens River (Stewart et al. 2005, Dettinger, 2013). The Eastern Sierra show signs of continued decline of regional snowpacks (Pierce et al. 2008, Tetra Tech, 2011), which also has significant economic and societal implications. In addition, extended droughts place significant pressure on water resources in the Sierra and may increase in frequency with warming climates (Dettinger, 2013). Mammoth Creek and the upper Owens River are the headwaters of this water supply, therefore it is important to thoroughly understand the linkages between climate and streamflow variability within these watersheds (Figures 1, 3). Climate and streamflow indices used in combination to evaluate drought and linkages to climate and hydrology at multiple time scales are particularly useful for evaluating watershed response and potential water resources for current and future periods (McKee et al. 1993; Vicente-Serrano et al. 2010).

The Standardized Precipitation Index (SPI), (McKee et al. 1993) and the Standardized Precipitation-Evapotranspiration Index (SPEI), (Vicente-Serrano et al. 2010), provide such quantitative climate indicators of drought frequency, magnitude and duration over a range of time scales. While the SPI assumes precipitation variability primarily controls drought characteristics, the SPEI also takes into account atmospheric

water demand through potential evapotranspiration (PET) estimates. Studies comparing the SPI and SPEI in the western United States suggest that accounting for temperature and potential evapotranspiration effects provides a better measure of drought severity and results in higher correlations between climatic and streamflow indices in basins receiving precipitation in the growing season (Abatzoglou et al., 2014; McEvoy et al. 2012; Wolf, 2010).

This thesis examines temporal relationships between climate and streamflow for Mammoth Creek, Hot Creek and the Upper Owens River, evaluates how results are related to headwater catchment geology, hydrogeology, and geochemistry, and provides some discussion points about potential future drought impacts and regional water resources. Empirical relationships between climate and streamflow are examined for Mammoth Creek, Hot Creek, and the Upper Owens River with the multi-scaler Standardized Precipitation Evapotranspiration Index (SPEI) at 12, 15, 24, 36, and 48-month timescales and standardized streamflows. The SPEI provides a useful basis for interpreting hydrologic regimes in this area because the impacts of climate variability on streamflow are multi-scaler and largely a function of the hydrogeology. Despite the importance of Mammoth Creek/Hot Creek and upper Owens River flows to the water supply of Los Angeles, detailed temporal relationships between climate variability and streamflow have not been described in the literature for the study area.

The general approach of this study relies on the use of the Parameter-Elevation Regression on Independent Slopes Model (PRISM; Daly et al. 1994) gridded temperature and precipitation data, and streamflow records to calculate SPEI and standardized streamflow indices (SSI) at a range of timescales. Correlations of SPEI

with SSI are used to determine the timescale of SPEI most closely related to surface water hydrology.

2. Environmental Setting

2.1 Regional Setting

The Sierra Nevada mountain range is the highest continuous mountain range in the United States. The range is a continuous cordillera extending 450 miles north to south along the eastern margin of California between 35° and 40° North latitude. The study area is located along the eastern escarpment of the Sierra drained by the Owens River that flows through the geologic provinces of the Sierra Nevada and the Basin and Range to its terminus, Owens Lake (Figure 1).

The Long Valley area lies on the western margin of the extensional Basin and Range Province and the major frontal faults of the Sierra Nevada batholith (Hildreth 2004; Mahood et al. 2010). The Long Valley Caldera area is a geologically young system capable of future volcanic activity as well as recurring earthquakes (Hill and others, 2001). A map showing the distribution of Quaternary faults in the Long Valley caldera is available at <http://earthquake.usgs.gov/hazards/qfaults/>. The Long Valley caldera is a tectonically active area; extensive surface rupture along the Hartley Springs fault caused property damage and injuries during four magnitude (M) ~ 6 earthquakes in May 1980 (U.S. Geological Survey, 2014).

The Long Valley caldera is one of three large magmatic systems in the United States that remain active today (Mahood et al. 2010), (Figure 2). The caldera erupted 760,000 years ago, ejecting an estimated 143.9 cubic miles (600 km²) of high-silica

rhyolite (Bailey 1989; Hildreth 2004). Subsequent eruptions from the Long Valley magma chamber included extrusions of rhyolite at 200,000-year intervals, forming thick sequences of fractured volcanic rock aquifers capable of storing large amounts of groundwater.

Mammoth Mountain lies west of the Long Valley caldera structural boundary and forms the southwestern boundary of the upper Owens River watershed (Figures 2, 3). Approximately 25 separate eruptive episodes between 110,000 and 57,000 years ago formed Mammoth Mountain (Hildreth 2004; Hildreth et al. 2014). Recent pyroclastic eruptions along the Mono-Inyo chain north of Mammoth Mountain produced extensive pumiceous and volcanic ash deposits with soil permeabilities ranging from 12 ft. to 40 ft. per day (NRCS, 1995). Permeability describes the ease with which gases, liquids, or plant roots penetrate or pass through a soil mass or layer (SSSA, 2001). Snowmelt infiltration is rapid and contributes to extensive groundwater recharge throughout the entire basin (Evans et al. 2002; Heim 1991; NRCS 1995; Tierney 2011).

The headwater cirques of Mammoth Creek and Hot Creek consist of impermeable granites and Tertiary metavolcanic rocks with areas of glacial till and alluvial deposits (Figure 3). During snowmelt runoff in the Mammoth Creek headwaters, the majority of snowmelt travels via shallow interflow and surface runoff to Mammoth Creek. Runoff derived from high-elevation snowmelt in the high elevation cirques of the Hot Creek watershed infiltrates into gravelly sandy soils on the alluvial fans at the base of the escarpment. The southern flank is composed of Pre-Tertiary igneous intrusive and metamorphic rocks and there is relatively little groundwater recharge in the crystalline-rock aquifers (Miller, 1999).

2.2 Previous Research on the Hydrology of the Long Valley Caldera

The Long Valley caldera supports an active hydrothermal system with numerous boiling hot springs and steam vents. The unique geologic and hydrologic resources of the area have been studied since J.D. Whitney's exploration in the 1860's. Israel Russell documented the geothermal resources of the Long Valley caldera in his 1889 report to the U.S. Geologic Survey (Russell, 1984). The prominent thermal springs near Casa Diablo in the Mammoth Creek watershed were described in a 1915 U.S. Geologic Survey water supply paper (Waring, 1915). Geothermal exploration contributed to understanding of the post caldera sequence of rhyolite eruptions. Borehole logs indicate a transmissive aquifer with water levels at approximately 600 ft. below ground surface. Permeability in the deep part of the well was related to fracturing of volcanic rocks while permeability in the upper part of the well was related to multiple stacked lava flows (Suemnicht 1987).

After a persistent swarm of earthquakes beneath Mammoth Mountain in 1989, geologists discovered large volumes of carbon dioxide (CO₂) gas issuing from soils on the slopes of the dormant volcano (Sorey et al., 1998; Stephens and Hering, 2002). Evans et al. (2002) attributed increased gas emissions to recent intrusions of magma under Mammoth Mountain. At the same time, the U.S. Geological Survey measured 50 tons per day of magmatic dissolved inorganic carbon (DIC) as CO₂ from cold water springs on the mountain and 10 tons per day at Big Springs (Evans et al. 2001; Farrar, 1999).

Using a variety of natural and anthropogenic tracers (Cl⁻, NO₃⁻), Evans et al. (2001) concluded the major cations formed by silicate weathering were the "strongest

geochemical evidence for flow from Mammoth Mountain to Big Springs” (Evans et al., 2001). SF₆ dating gave a minimum age estimate of about 12 years for Big Springs (Evans et al. 2002). These findings established the presence of long flowpaths in permeable, thick sequences of fractured and layered volcanic rocks and confirmed the permeability and stratigraphy found in geothermal exploratory wells (Suemnicht 1987).

Kondolf and Vorster (1992) noted large-scale streamflow-groundwater interactions in the Deadman Creek – upper Owens River watershed. Following snowmelt recession, streamflow in Deadman Creek was lost to infiltration due to highly permeable pumiceous soils in the west moat, speculating that infiltrated groundwater contributed to flow at Big Springs.

Competing demands for surface and groundwater resources in the Mammoth Lakes Basin prompted hydrologic research on developing conceptual models of the groundwater basins and exploring potential connections between groundwater pumping in the Town of Mammoth Lakes and the Hot Creek Fish Hatchery Springs (USGS 2010; Wildermuth, 1996, 2003). Other recent research investigated the relationship between groundwater pumping and streamflows in Mammoth Creek and the Hot Creek Fish Hatchery springs. Burak et al. (2006) found groundwater pumping during low streamflow periods were related to decreases in stream discharge (Burak et al. 2006; Custis, 2008). Wildermuth (1996; 2003) concluded groundwater extraction for golf course irrigation in the central part of the Mammoth groundwater basin did not affect spring discharge at the Hot Creek Fish Hatchery Springs.

Major ion chemistry and isotope samples collected from 2008 to 2011 from Big Springs, Deadman Creek and springs on the San Joaquin Ridge showed high K⁺/Na⁺

and Mg^{+2}/Na^{+} ratios typical of the earliest stages of rock weathering ((Burak, 2010, Appendix A; Evans et al. 2002; Hem, 1985; Kehew, 2000). Stable isotopes of deuterium (D) and oxygen 18 (^{18}O) plotted on or close to the Global Meteoric Water Line (Craig, 1961) for surface waters in the Mammoth Basin and upper Owens River watershed and groundwater samples indicated meteoric water sources with little or no evaporation.

2.3 Local Setting

Mammoth Basin

The Mammoth Hydrologic Basin encompasses the Mammoth Creek and Hot Creek watersheds (Figure 4). The Mammoth Basin watershed is 46,697 acres with diverse topography characterized by elevations ranging from 6,900 ft. in the central portion of the Long Valley caldera to over 12,500 ft. on Bloody Mountain on the Sierra Crest (Figures 4, 5). The Mammoth Basin watershed includes the Mammoth Creek and Hot Creek watersheds: the Mammoth Creek watershed is 21,632 acres (33.8 mi²) and contains the glaciated granitic headwater cirques of Mammoth Creek.

The Mammoth groundwater basin lies within the central region of the Mammoth Basin (Figure 5). The central region opens and drains to the east and south to Crowley Lake (Wildermuth, 1996, 2003). Boundaries of the groundwater basin are undefined because of the complex geology and hydrogeology of the Mammoth Basin watershed (Wildermuth, 2003, Wildermuth 2009). Based on cross sections passing through the Mammoth Community Water District's well fields, a shallow, transmissive system of glacial till and alluvium responds rapidly to recharge and a deeper system consisting of

alternating layers of fractured basalts, glacial till, and alluvial material responds slowly to recharge (MCWD, 2005).

Soils are generally shallow, poorly developed and often limited to topographic benches in steep granitic headwater cirques. Gravelly loams with low water capacity are found on glacial outwash and on glacial moraines. Soil permeabilities range from 4 to 12 feet per day in gravelly loams and 12 to 40 feet per day in areas of glacial deposits (NRCS 1995).

The Hot Creek watershed drains the steep Sierra escarpment on the southern boundary of the watershed. The portion of the watershed located on the floor of the Long Valley caldera consists of outcrops of fractured basalt and rhyolite flows and gravelly sandy soils. A large rhyolite flow informally known as the Hot Creek Flow forms the eastern boundary (Bailey 1989). Soil permeabilities range from 12 to 40 feet per day (NRCS 1995). The headwaters of Hot Creek are high volume thermal springs discharging from fractured basalt flows along the south side of the hatchery. Water discharged from the springs is a mixture of cold shallow groundwater recently recharged from snowmelt and thermal groundwater. Mammoth Creek combines with Hot Creek at the Hot Creek Fish Hatchery springs.

Downstream from the hatchery springs, Hot Creek enters the Hot Creek Gorge eight miles east of the town of Mammoth Lakes where numerous hot springs add hot water into the stream. Combined flows of Mammoth and Hot Creek contribute 25 to 30 per cent of the city of Los Angeles Department of Water and Power's annual water export from the Eastern Sierra (MCWD, 2010).

Mammoth Creek flows are measured at the Old 395 DWP gage (Figures 1, 4, Table 3). Mean annual runoff of Mammoth Creek for the period of record 1951 to 2011 is 16,472 ac-ft. per year. Mean monthly discharge is 23.5 cfs. Snowmelt runoff generated in spring and early summer produces peak streamflow in June and July, followed by steep declines in discharge as more streamflow is derived from groundwater storage (Figure 6); (Peterson et al. 2003, Singh and Singh 2001). Snowmelt runoff in the Mammoth Creek watershed above the DWP 395 gage generates 70 percent of mean monthly discharge with about 30 percent of mean monthly discharge contributed by groundwater. Mammoth Creek becomes Hot Creek at the point where the Hot Creek Fish Hatchery springs contribute flow to the stream. Mean annual runoff of Hot Creek measured at the USGS Hot Creek Flume is 43,980 ac-ft. per year (Figures 1, 4, Table 3). Mean monthly discharge is 60 cfs. Prudic (email comm. 2013) estimated about 83 percent of mean discharge measured at the Hot Creek Flume is groundwater.

Upper Owens River Basin

The upper Owens River watershed is 47,729 acres in size, with topographic relief ranging from 11,500 ft. along the western boundary of the watershed along the San Joaquin Ridge to 7,104 ft. at the East Portal gage on the northern margin of the Long Valley caldera (Figure 2). The upper Owens River flows east and south along the northern boundary of the Long Valley caldera to the confluence with Hot Creek; combined flows meander for four miles until reaching the Crowley Lake reservoir, the largest reservoir on the 183- mile reach of the Owens River (Figure 2).

Mean annual runoff from the upper Owens River watershed is 42,360 ac-ft. per year as measured at the DWP East Portal gage (Table 1). Deadman Creek drains the upper watershed and flows during snowmelt runoff. A complex of high volume springs known as Big Springs form the perennial headwaters of the upper Owens River at 7,000 ft. along the northern boundary of the Long Valley caldera (Figure 1, 2). The ground surface is highly permeable to infiltration; as a result, there is little direct snowmelt runoff (Evans et al. 2002). Mean monthly discharge is 58.9 cfs with snowmelt runoff generating about 16 to 20 percent of mean monthly discharge with about 80 to 84 percent contributed by groundwater (Prudic, email comm. 2013). Groundwater in the upper Owens River watershed is assumed to move from areas of recharge on Mammoth Mountain and the San Joaquin Ridge to Big Springs along a hydraulic gradient that follows the land surface slope and the northeast orientation of numerous faults (TEAM, 2007).

Recharge for the groundwater system is believed to occur to the west and southwest in the watersheds of Deadman Creek and Dry Creek (Kondolf and Vorster 1992, Evans et al. 2001; Evans et al. 2002). Groundwater flowing from Mammoth Mountain is diluted by snowmelt that accumulates on the caldera flow and by groundwater flowing in from the western rim of the caldera (Evans et al. 2001). A second aquifer system likely exists in the Tertiary lavas that cap the San Joaquin Ridge; isotopic signatures indicate springs are derived from snowmelt and combine to form the headwaters of Deadman Creek. Kondolf and Vorster (1992) suggested groundwater migrated through pumice and deeper fractured basalts and rhyolites to the low gradient slopes in the west moat and Deadman Creek streamflow infiltrates and flows

underground following snowmelt recession, presumably to Big Springs (Kondolf and Vorster, 1992). Deadman Creek snowmelt runoff flows range from one to 121 cfs in 1991 and 2011 respectively (USFS, unpublished data, Burak, unpublished data). Big Springs discharge is a minor contribution to flow during high snowmelt but is the dominant source of streamflow in late summer and fall.

Dry Creek originates from a small spring on the north slopes of Mammoth Mountain; a portion of flow is diverted into a man-made snowmaking pond; during snowmelt runoff, surface flow continues downstream on the lower slopes of Mammoth Mountain until surface flow is lost via a combination of evaporation and infiltration (TEAM, 2007).

2.4. Climate

Approximately 85 to 90% of annual precipitation in the Sierra Nevada results from storms that originate over the Pacific Ocean from October through April (DWR, 1973; Cayan 1996; Dettinger et al. 2004). Pacific storms funnel from the southwest up through the San Joaquin River canyon through the relatively low gap in the Sierra Crest at Mammoth Mountain. Strong zonal westerly flow and orographic enhancement brings large volumes of snow to the area (Losleben et al. 2001), reducing the rain shadow effect typical of eastern slope of the Sierra Nevada (Howald 2000a). Mean April 1 snow water equivalence (SWE) at the Bureau of Reclamation Mammoth Pass station (MHP, Table 3) is 42.5 inches. Mean annual precipitation ranges from more than 50 inches along the Sierra Crest to less than 10 inches at the Crowley Lake Dam 15 miles east of the Mammoth Pass station near the southeastern boundary of the caldera (Table 2).

Climate is the major source of variability in the timing and amount of streamflow (Peterson et al. 2003; Stewart et al. 2008). The seasonality of streamflow also varies due to differences in soil thickness and storage potentials, infiltration capacity, duration of infiltration period, and mountain block permeability (Wildermuth, 2003). Variability in the response of streamflow to seasonal precipitation is shown in departure from mean annual streamflow plots for the period 1951-2011 (Figures 7, 8, 9). The variability of Mammoth Creek streamflow at the DWP 395 gage exhibit a high coefficient of variation of 1.4 (Table 3) compared to groundwater dominated streamflow of Hot Creek and the upper Owens River (coefficient of variation 0.49 and 0.24, respectively).

3. Methods

3.1 Climate data

PRISM (Parameter-elevation Regressions on Independent Slopes Model) uses point data, a digital elevation model (DEM) and other spatial datasets to generate gridded estimates of annual, monthly and event-based climatic parameters (Daly et al. 1994). Monthly gridded datasets of total precipitation and maximum and minimum temperature at 800-meter spatial resolution for the period of record from 1951 to 2011 were partitioned into sub basins of the Mammoth Creek and the upper Owens River watersheds. Drought indices were calculated for each stream-gage site using spatially averaged 800-meter-by-800-meter PRISM pixels within the upstream drainage.

3.2 Hydrologic data

Continuous daily streamflow records were obtained from gauging stations located on Mammoth Creek and the upper Owens River from the U.S. Geologic Survey (USGS), the Los Angeles Department of Water and Power (DWP) and the Mammoth Community Water District (MCWD). Streamflow gage and watershed characteristics are summarized in Tables 1 and 3. Daily streamflow records from water year 1951 to 2011 were examined and corrected for missing values anomalous values due to streamflow gage icing, and then aggregated into monthly time steps; monthly time steps were aggregated into annual runoff. Time series of streamflow were standardized using the log-logistic distribution following Vicente-Serrano et al. (Vicente-Serrano et al. 2010). The standardized hydrologic time series were correlated with each watershed SPEI time series at multiple time scales and evaluated using Pearson's linear correlation coefficient (Vicente-Serrano and Lopez-Moreno, 2005).

To evaluate the range of streamflow at each site the 15-day running median was calculated for the wettest and driest years of record following Godsey et al. (2013). High and low-flow periods were defined as the range of days that daily discharge remained below the 25th percentile and above the 75th percentile of all historical flows (Figures 10,11,12). Using fifteen-day running median daily streamflow minimized the effect of individual, potential outlier values in the streamflow time series.

3.3 Calculation of SPEI

The SPEI incorporates the effects of evaporative demand through the estimation and incorporation of PET into a simple water balance. PET was calculated using the

Thornthwaite approach based on PRISM generated average monthly temperature (T) and latitude used to estimate the length of daylight (Thornthwaite, 1948; Appendix A). The physically based Penman-Monteith method (Allen et al. 1998) has been shown to be more appropriate for drought impact studies (Hobbins et al. 2012), however the Penman-Monteith method requires solar radiation, temperature, wind-speed, and relative humidity data and was not available for the study watersheds for the entire period of record.

The difference between precipitation and potential evapotranspiration (P-PET) provides a measure of the water surplus or deficit for each month. The time scale over which P-PET deficits and surpluses accumulate separates meteorological, hydrological, agricultural, and socioeconomic drought (Lorenzo-Lacruz et al. 2013). Once P-PET is determined from the Thornthwaite equation, the difference between monthly precipitation P and PET is calculated (Appendix B). Monthly P-PET differences were aggregated at different time scales, quantifying the natural lags between precipitation and the arrival of streamflow at the streamflow gage (Vicente-Serrano and Lopez-Moreno, 2005). P-PET values are either positive, indicating water surplus, or negative, indicating water deficits for each analyzed month. For this study, P-PET values were aggregated at the 12, 15, 24, 36, and 48-month time scales.

The SPEI fits precipitation, P-PET and streamflow data to a log-logistic distribution using L-moments (Appendix B). Probabilities were standardized using an inverse normal function following the work of Vicente-Serrano et al., (2010) with a mean of zero and standard deviation of one. The magnitude of the departure from zero

indicates the severity of drought or periods of above mean precipitation (Table 4, Guttman, 1999).

The SPEI was calculated at time scales of 1, 12, 15, 24, 36, 48, 72, 96 and 108 months; results from the 15, 24, 36 and 48-month timescales were used in the correlation analyses with standardized streamflow. Since streamflow response to drought of the different systems were not known, the Pearson correlation coefficient r between streamflow and the 1 to 48-month SPEI series was computed, and the time scale at which the strongest correlation was found was kept for further analyses (Vincente-Serrano et al. 2012). Time series of SPEI and standardized streamflow for each watershed illustrate the frequency and magnitude of wet and dry periods for each watershed (Figures 16, 17, 18).

4. RESULTS

4.1 Geologic and hydrologic relationships

Streamflow in Mammoth Creek exhibits greater departures from mean annual flow than Hot Creek and the upper Owens River (Figures 7, 8, 9). Snowmelt runoff in 1983 approached 200 percent of mean annual streamflow, while streamflows on Hot Creek and the upper Owens River approached 75 percent of the mean. A series of dry winters from 1987 to 1994 resulted in negative values of -30 to -40 percent on the upper Owens River and Hot Creek while Mammoth Creek departures approached -75 percent. These results highlight the unique aquifer storage and groundwater discharge characteristics of the upper Owens River and Hot Creek watersheds.

Figures 10, 11, 12 illustrate differences in the variability and seasonal distribution of streamflow. Spatial patterns exhibit significant differences between surface and shallow subsurface flow through poorly developed soils in the Mammoth Basin headwaters and the slow draining basaltic aquifers in the west moat of the Long Valley caldera. Mammoth Creek and Hot Creek hydrographs show a rapid response to snowmelt runoff because interflow takes infiltrated snowmelt to the stream relatively quickly. The recession limb on Mammoth Creek is steep, falling to 10 cfs by September. When Mammoth Creek flows decline to 4.5 cfs as measured at the DWP 395 gage, regulations prohibit surface water diversions from Mammoth Creek and groundwater provides domestic water supplies for the Town of Mammoth Lakes.

Hot Creek's recession limb gradually declines to around 55 cfs due to groundwater inputs from the Hot Creek Fish Hatchery springs. Snowmelt response is delayed and attenuated on the upper Owens River due to the large component of groundwater discharge from Big Springs. Minimum streamflows occur earlier in dry years than in wet years in the watersheds. Snowmelt runoff in dry years shows a small peak on the Upper Owens River due to lack of snowpack accumulation in the west moat and minimal contributions from Deadman Creek.

4.2 SPEI

Figures 13 and 14 illustrate SPEI at the 12, 24, 36, and 48-month timescales. The 12-month timescale reflects the influence of interannual precipitation with high frequency and short duration periods compared to longer timescales. At the 12-month timescale, the dry (SPEI <0) and wet (SPEI >0) periods show high temporal frequency.

To identify the main dry periods, it is necessary to Analysis of longer timescales is necessary to identify the main dry periods because the high frequency of SPEI at short timescales hide the most important dry periods (Vicente-Serrano and Lopez-Moreno, 2005). At longer timescales, dry and wet periods persist for longer periods and are somewhat less in magnitude due to longer aggregation and smoothing effects. At the 48-month timescale only three important dry periods (SPEI <-1) are recognized: the decade of 1960, the 1970's, and 1987 to 1994. Trends of increasing drought frequency and severity documented by many authors (e.g., Abatzoglou et al. 2014; McEvoy et al. 2012; Vicente-Serrano 2010; Vicente-Serrano et al. 2011) are not evident.

4.3 SPEI and Standardized Streamflow

Figure 15 shows the Pearson correlation coefficient between continuous standardized series of stream discharge and the SPEI time series at different timescales. At shorter timescales, the relationship is poor- at the two –month timescale, the correlation is only $r = <0.1$. The correlation increases as the timescale increases, with a maximum of $r = 0.77$ and $r = 0.67$ on Mammoth Creek and Hot Creek at the 15-month timescale. Maximum correlation of $r = 0.67$ occurs at the 48-month timescale on the upper Owens River and the low slope of the curve indicates the strong influence of groundwater discharge to the stream.

Figures 16, 17, and 18 illustrate standardized streamflow and optimal timescale SPEI time series for the upper Owens River and the Mammoth Basin watersheds. As expected based on the geology and hydrogeologic characteristics, the high frequency signal of the SPEI at the 15 and 24-month timescale is not well correlated with

streamflow in the upper Owens River (Figure 16). The lower frequency signal of SPEI at the 36 and 48-month timescale is better correlated with streamflow; however streamflow and SPEI signals diverge in 1974 to 1976 and from 1978 to 1979. SPEI indicates dry conditions from 1973 through 1980 despite average and above average monthly and annual streamflows in 1973, 1974 and in 1978 to 1981 (Figure 7). Both indices are negative in 1976 and 1977. Standardized monthly streamflow does not accumulate so the comparison is between monthly streamflow and deficits of P-PET aggregated over the previous 48-months. The longer timescales of SPEI are not sensitive to monthly variations in streamflow and disparities result when streamflows vary on an annual basis.

SPEI values change sign in the 1980 runoff season at Hot Creek and the upper Owens River (Figure 16, 18). Higher correlations between SPEI and SSI occur from 1981 through 1986 when streamflow and SPEI indicate wet conditions. PET values during this time-period were lower due to abundant precipitation and aggregated P-PET was positive, corresponding to above average streamflows.

Groundwater dominated systems of upper Owens and Hot Creek are less sensitive to variability of precipitation due to large area of recharge, groundwater storage, and higher volumes of groundwater discharge; upper Owens River streamflow was 5 percent above mean annual streamflow in 1987, the first year of severely dry conditions in the 1987 to 1994 drought (Figures 7, 16). Hot Creek streamflow responded to very low precipitation in 1987 because Mammoth Creek was minus 50 percent of the long term mean (Figure 9).

4.4 Monthly Correlations between SPEI and standardized streamflow

Figures 19, 20 and 21 illustrate r-Pearson correlations between standardized streamflow and monthly SPEI values for each time scale and month. Mammoth Creek and Hot Creek exhibit the highest correlations (0.91 and 0.87) at the 8 to 15-month timescale in July during snowmelt recession (Figures 20, 21) when temperatures are above freezing and PET becomes more important to the local hydrology (PET ~ 4.0 inches per month); (Wolf, 2010). SPEI and streamflow are poorly correlated ($r < 0.3$) during the fall and winter baseflow period when temperatures are below freezing, plants are dormant (PET = 0) and precipitation events are frequent.

The highest monthly correlations between SPEI and streamflow ($r = 0.76$) occur at the 36 to 60-month timescale in September in the upper Owens River watershed (Figure 19). High correlations between monthly streamflow and SPEI also occur at the 8 to 15 month timescale, reflecting Deadman Creek snowmelt runoff contributions to the upper Owens River above Big Springs. Correlations remain above 0.6 for the fall and winter months at longer time scales of 24 to 48 months due to groundwater held in storage.

5. Discussion

Variations in geology across the study area influence the timescales of hydrologic response to climate, as illustrated with correlations between SPEI and standardized streamflow. Differences in hydrologic response times suggest there are distinct catchment characteristics including topography, geology, soils, and vegetation that influence hydrologic travel times in each watershed (Tague and Grant, 2004).

Contributions from groundwater-dominated streams are an important component of flow during the driest part of the year and during the driest years for water supply and fisheries (Mayer and Naman 2011).

Hydrographs illustrate the transition from the rapid hydroclimate response of upstream Mammoth Creek to the groundwater-dominated flows on Hot Creek. Limited groundwater storage results in low summer and fall flows that limit surface water availability for fisheries and domestic water supply on Mammoth Creek. In contrast, snowmelt infiltrates into pumice soils on the slopes of Mammoth Mountain and the San Joaquin Ridge, percolating through stacks of permeable volcanic rock layers to deep water tables then travels along basalt flows in the west moat of the Long Valley caldera to discharge at Big Springs. Flow between Mammoth Mountain and Big Springs is supported by the order of magnitude decline in DIC between Mammoth Mountain and Big Springs (Evans et al. 2001). Cations released by silicate weathering of volcanic rocks also provide strong evidence for flow from Mammoth Mountain to Big Springs (Evans et al. 2001; Appendix A).

The age estimate of ~ 12 years obtained for Big Spring from SF₆ dating suggest long flowpaths in the upper Owens River watershed are responsible for the delayed response between climate and streamflow. Longer timescales are related to higher watershed permeability and greater aquifer storage properties (Vincente-Serrano et al. 2010). Isotopic signatures of Mammoth Creek confirm surface waters are derived from winter storms, supporting the close relationship between 15-month SPEI timescales and streamflow. High correlations are also related to shallow interflow, low soil water holding capacity and low aquifer storage potential. SPEI and standardized streamflow

generally track each other inter-annually and successfully captured dry and wet events for Mammoth Creek ($r = 0.77$) and to a lesser degree for the Hot Creek and upper Owens River ($r = 0.67$), (Figures 16, 17, 18). Periods of opposing signs of SPEI and streamflow occur more frequently on the upper Owens River and Hot Creek than on Mammoth Creek. Accumulated surpluses or deficits of P-PET aggregated at different time scales contrast with monthly-standardized streamflow when variability of precipitation is high on monthly timescales. For a given year and month, streamflow may be above average due to combined inputs of precipitation and groundwater discharge in the upper Owens River and Hot Creek watersheds but if precipitation is below average in individual years, aggregated P-PET deficits result in $SPEI < 0$. The SPEI is a statistical model and relationships between accumulated P-PET over different timescales and monthly streamflow may not explain the physical process of snowmelt infiltration, percolation, and travel time to a single point of discharge.

The Thornthwaite approach assigns values of zero to PET when temperatures are below freezing and the monthly water balance is positive. During the runoff and low flow season, there is little precipitation and P-PET is negative because temperatures and evapotranspiration are high and negative values of P-PET occur much more frequently. . It is not clear if the Penman-Monteith approach would significantly alter the sign of the monthly water balance and result in higher correlations between SPEI and streamflow.

The parameterization of PET using Thornthwaite has limitations that might influence SPEI values; Hobbins et al. (2012) found temperatures were not always the most significant driver of temporal variability in evaporative demand, particularly at seasonal time scales. Depending on the region and season, temperature, specific

humidity, incoming solar radiation, and wind speed could be the main drivers of evaporative demand. Hobbins et al. (2012) concluded temperature and latitude could not be used to capture the variability of radiation and may not be suited in mountainous terrain. Additionally, ordinary least squares regression compared PRISM-modeled temperatures (<http://www.prism.oregonstate.edu/explorer/>) to observations from stations listed in Table 2. PRISM temperatures were 1^o to 2^o F higher than station values for the period of record suggesting the parameterization of PET using PRISM modeled temperature could influence SPEI values.

Trends of increasing drought severity are not observed; however, other studies suggest that drought severity will increase in high elevations as snowlines increase and areas that usually snow-covered are bare (Hidalgo et al. 2006). The inclusion of atmospheric demand using the Thornthwaite approach appears to be less useful for characterizing drought in the study watersheds where mean annual precipitation is much greater than in the arid regions of the eastern Sierra Nevada and the Great Basin in Nevada (McEvoy et al., 2012).

6. Conclusions and Future Work

This study examines hydrologic response to climate associated through the use of standardized streamflow and SPEI time series (Vicente-Serrano et al. 2010). While annual variability in streamflow is largely a function of the amount of water stored in the snowpack (Dettinger, 2004; Nippgen et al. 2011; Prudic 2013), climate and hydrologic response analysis through the use of SPEI analyzed at different time scales suggest that seasonal and annual hydrologic response are largely controlled by the

geology within the watershed. The timescales of SPEI that are highly correlated to standardized streamflow are 15-months for the Mammoth Basin watershed and 48-months for the upper Owens River watershed (Figure 15). High correlations in June and July at shorter timescales in the upper Owens River watershed (Figure 19) suggest snowmelt is partitioned into shallow pumiceous aquifers that respond to seasonal snowmelt runoff from Deadman Creek and deeper, highly transmissive volcanic aquifers that slowly transmit water throughout the year. The period of higher correlations ($r > 0.70$) at the 48 and 60-month timescale, suggest deep aquifers are the source of perennial spring discharge at Big Springs. Longer time scales indicate groundwater modulates the yearly climate signals though the temporal constraints on groundwater discharge are not known.

The discharge of large amounts of groundwater at a single point such as Big Springs requires a combination of large recharge area, a high recharge rate and laterally extensive, interbedded and highly transmissive volcanic aquifers (Manga, 2001). Numerous springheads at Big Springs occur at the base of a basalt flow with groundwater originating from Mammoth Mountain. Groundwater flow is constricted when it approaches the ground surface after traveling long distances through layers of fractured lava flows (Hildreth, 2004, Hildreth et al. 2014). The age estimate of 12 years for Big Springs supports the conceptual model of large aquifer storage and long residence times. Longer SPEI timescales (i.e. 48 months) for Big Springs also support this conceptual model, but is much shorter because it is based on climate and hydraulic responses.

The highest monthly correlations between streamflow and SPEI on Mammoth Creek and Hot Creek occur at the 6 to 15-month timescale and illustrate a rapid hydroclimate response of relatively impermeable granitic aquifers to snowmelt runoff (McEvoy et al. 2012). Granites and metasedimentary rocks with limited permeability and groundwater storage capacity (Price, 2009; Tague et al. 2008) underlie the headwater cirques of Mammoth Creek. These findings have implications for water management in the Mammoth Creek watershed because lack of groundwater storage in the headwater catchments increases reliance on groundwater extracted from the Mammoth Groundwater Basin to supply domestic water during dry periods.

These results paired with the hydrogeologic setting of the watersheds suggest that the relatively impermeable granitic mountain block watershed of Mammoth Creek limits deep subsurface flow and groundwater storage, while more permeable volcanic rocks of the upper Owens River allow for deep groundwater recharge, storage, and sustained baseflow. Silicate weathering of volcanic rocks, age dating of water and naturally occurring isotopes of water support the timescales identified by the SPEI. Findings from this study highlight and reaffirm the lesser-known multi-time scale linkages between climate variability, hydrogeology, and hydrologic regimes of Mammoth Creek, Hot Creek and the upper Owens River using drought and streamflow indices.

Future work

California continues to experience severe widespread drought conditions that began after the end of the study period from 2012 to the present. Mammoth Creek and the upper Owens River are flowing at historic lows. The SPEI and streamflow analyses

in this study should be extended to include the ongoing drought conditions. Evaporative demand is likely playing a larger role with above average monthly temperatures recorded at stations in the study area from 2012 to the present. Estimating PET using the physically based Penman- Monteith approach is also necessary to evaluate the drivers of evaporative demand and impacts of drought. The influence of increasing temperatures on snowlines and SWE: P ratios would identify changes in the seasonality of precipitation and the fraction of precipitation falling as snow.

Low spatial resolution of data sources in the study area and the heterogeneity of the landscapes in the watersheds limit the ability of PRISM precipitation and temperature datasets to reflect climatic conditions that occur at specific locations and for specific storms (Lundquist et al., 2010). Regions without major terrain features and located inland of the Pacific coast can be handled adequately by most interpolation techniques (Daly, 2006); the eastern Sierra is characterized by steep elevation gradients, rain shadow and cold air drainage and PRISM data should be augmented with independent data sources (Daly, 2006). Utilizing meteorological station data from Mammoth Mountain, the Mammoth Lakes airport and the Sierra Nevada Aquatic Research Lab (SNARL) would likely provide independent data that might reduce interpolation errors.

Groundwater extraction in the upper Dry Creek sub watershed increases each year as a result of ski area expansion and snowmaking at Mammoth Mountain Ski Area. During the 2012 through 2015 winter seasons, Mammoth Mountain Ski Area used large volumes of groundwater for snowmaking to augment sparse natural snowcover from late October to February. During this time, snowmaking wells went dry in the upper Dry

Creek drainage. Considering groundwater-pumping impacts on surface water would be a complementary analysis for future drought and hydroclimate investigations.

Evans et al. (2001) traced higher than natural background concentrations of Cl^- and NO_3^- to the application of NaCl and NH_4NO_3 on the slopes of Mammoth Mountain to improve spring skiing. Monitoring Cl^- and NO_3^- concentrations in future work would provide further evidence of a hydrologic connection as ski area operations continue to expand (Evans et al., 2001).

A better understanding of recharge volumes and groundwater flowpaths in the upper Owens River watershed is needed to evaluate potential impacts to Big Springs discharge and upper Owens River flows from current and proposed future groundwater pumping (Bren 2002; Forest Service 1994; Kondolf and Vorster 1992; TEAM, 2007). The upper Owens River watershed, the Mammoth Basin watershed, and the adjacent Mono Basin supply the majority of water transported to the City of Los Angeles. Estimating groundwater recharge and storage in the basins, and implementation of a groundwater management plan are essential to protect water supplies during prolonged drought.

The effects of a changing and warming climate pose an uncertain future for local water supply and economies based on winter and summer recreation. In an area where summer streamflow and groundwater discharge are essential for water supply and fisheries during times of the year with high evaporative and ecological demands, understanding relationships between snowmelt timing, streamflow and groundwater interactions will assist local agencies to address climate change impacts on hydrologic resources in the region. The results from this work can complement future studies

focused on relationships between climate, streamflow, groundwater recharge and discharge, and drought.

Literature

Abatzoglou, J., Barbero, R., and J.W. Wolf (2014). Tracking Interannual Streamflow variability with Drought Indices in the U.S. Pacific Northwest, *J. Hydrometeorology*, 2014.

Ahmad, M.I., C.D. Sinclair, and A. Werrity (1988). Log-logistic flood frequency analysis. *Journal of Hydrology* 98, 205-224.

Allen, R. G., L. S. Pereira, D. Raes, and M. Smith (1998). Crop evapotranspiration: Guidelines for computing crop water requirement. Food and Agricultural Organization of the United Nations Irrigation and Drainage Paper 56, 300 pp.

Bailey, R.A. (1989). Geologic Map of Long Valley Caldera, California, Mono Craters Volcanic Chain and Vicinity, Eastern California. U.S. Geol.Surv. Map I-1933, 1989.

Bailey, R.A.(2004). Eruptive History and Chemical Evolution of the Precaldera and Postcaldera Basalt-Dacite Sequences, Long Valley, California: Implications for Magma Sources, Current Seismic Unrest and Future Volcanism. U.S. Geol. Survey Prof. Paper 1692 75 pp.

Breibart, A.D., R.E. Cathcart, K.A. Didriksen, and J.L. Everett (2001) Mammoth Groundwater Extraction: A Hydrological Analysis of Potential Recharge to an Eastern Sierra Nevada Watershed. Donald Bren School of Environmental Science and Management, University of California, Santa Barbara.

Burak, S. (2006). Preliminary Evaluation of a Hydrologic Connection Between Mammoth Creek and Mammoth Community Water District Water Supply Wells, Mono County, California. Professional Report to Mammoth Community Water District, 67 pp.

Burak, S. (2010). Preliminary Geochemical Assessment, Big Springs, Mono County, California. Internal report prepared for California Trout, Inc.

California Department of Water Resources (1973). Mammoth basin water resources environmental study (final report), DWR Southern District, Sacramento.

Daly, C. (2006). Guidelines for assessing the suitability of spatial climate data sets, *International Journal of Climatology*, 26: 707-721.

Cayan, D. R. (1996). Interannual climate variability and snowpack in the western United States. *Journal of Climate*, 9.

Chen, R., Branum, D. M., Wills, C. J. and D. P. Hill, Scenario Earthquake Hazards for the Long Valley Caldera-Mono Lake Area, East-Central California, U.S. Geological

Survey Open-File Report 2014-1045, and California Geological Survey Special Report 233, 92 p.

Clark, I and P. Fritz. (1997). *Environmental Isotopes in Hydrogeology*. Lewis Publishers, New York.

Craig, H. (1961). Isotopic variations in meteoric water. *Science*, v.133, no. 3465.

Custis, K.(2008). Preliminary Evaluation of Hydrogeologic Setting and Impacts on Mammoth Community Water District Groundwater Extraction on Surface Water Flows in Mammoth Creek, Mammoth Lakes, California. Memorandum, State of California Department of Fish and Game.

Daly, C., Neilson, R.P. and D.L. Phillips (1994). A statistical-topographic model for mapping climatological precipitation over mountainous terrain. *J. Appl. Meteor.*, 33, 140-158.

Daly, C. (2006). Guidelines for assessing the suitability of spatial climate data sets, *International Journal of Climatology*, 26: 707-721.

Danskin, W.R. (1998). Evaluation of the Hydrologic System and Selected Water-Management Alternatives in the Owens Valley, California. U.S. Geological Survey Water-Supply Paper 2370-H.

Department of Water Resources, California Data Exchange Center,
<http://cdec.water.ca.gov/>

Dettinger, M.D. and D.R. Cayan (1995). Large scale forcing of recent trends towards earlier snowmelt runoff in California, *J. Climate*, no. 8, 606-623.

Dettinger, M.D., Redmond, K.T., and Cayan, D.R. (2004). Winter orographic-precipitation ratios in the Sierra Nevada—Large-scale atmospheric circulations and hydrologic consequences: *J. Hydrometeorology*, 5, 1102-1116.

Evans, W. C., Sorey, M. L., Michel, R. L., Cook, A. C., Kennedy, B. M., and Busenberg, E., (2001). Tracing magmatic carbon in groundwater at Big Springs, Long Valley caldera, USA, in Cidu, R., ed.: *Water-Rock Interaction-10*, Cagliari, 2001, p. 803-806.

Evans, W.C., M. Sorey, A.C. Cook, B.M. Kennedy, D. Shuster, E. Colvard, L. White and M.A. Huebner (2002). Tracing and quantifying magmatic carbon discharge in cold groundwaters: Lessons learned from Mammoth Mountain, USA. *Journal of Volcanology and Geothermal Research* 114 (2002) 291-312.

Farrar, C.D., Neil, M.N., and J. F. Howle. (1999). Magmatic Carbon Emissions at Mammoth Mountain, California. U.S. Geological Survey Water Resources Investigations Report 98-4217.

Godsey, S.E., J.W. Kirchner and C.L. Tague. (2013). Effects of changes in winter snowpacks on summer low flows: case studies in the Sierra Nevada, California, USA. *Hydrological Processes*, 28, 5048-5064.

Heim, K. (1991). Hydrologic Study of the Upper Owens River Basin Big Springs to East Portal, (unpub.rep.), California State University, Fullerton.

Hidalgo, H.G., Cayan, D.R. and M.D. Dettinger. Drought- how the western U.S. is transformed from energy-limited to water-limited landscapes, *J. Hydromet.*, May 2006.

Hildreth, W. (2004). Volcanological perspective on Long Valley, Mammoth Mountain and Mono Craters: several contiguous but discrete systems: *Journal of Volcanology and Geothermal Research*, v. 136, p. 169-198.

Hildreth, W., Fuerstein, J., Champion, D and A. Calvert (2014). Mammoth Mountain and its mafic periphery- A late Quaternary volcanic field in eastern California. *Geosphere*, published online on 12 November 2014, doi: 10.1130/GES01053.1.

Hill, D.P. (1996). Earthquakes and carbon dioxide beneath Mammoth Mountain, California: *Seismological Research Letters*, v. 67, no. 1, p. 8-15.

Hobbins, M., Wood, W., Struebel, D., Werner, K.(2012). What Drives the Variability of Evaporative Demand across the Conterminous United States? *J. Hydrometeorology*, V. 13, pp. 1195-1214.

Hosking, J. R. M., and J. R. Wallis. (1986). The Value of Historical Data in Flood Frequency Analysis, *Water Resour. Res.*, 22(11), 1606–1612.

Hosking, J.R.M. (1990). L-Moments: Analysis and estimation of distributions using linear combinations of order statistics. *Journal of Royal Statistical Society B*, 52: 105-124.

Howald, A. (2000a). Vegetation and Flora of the Mammoth Mountain Area, A Partial Checklist of the Vascular Plants of the Mammoth Mountain Area, Mono and Madera Counties, California. Museum of Systematics and Ecology, University of California, Santa Barbara.

Kondolf, M. and P. Vorster. (1992). Management Implications of Stream/Groundwater Interactions in the Eastern Sierra Nevada, California. In, *The History of Water: East Sierra Nevada, Owens Valley, White-Inyo Mountains*. Eds. C.A. Hall, V. Dole Jones and B. Widawski, University of California, White Mountain Research Station, Symp. Vol 4..

Lorenzo-Lacruz, J., Moran-Tejada, E., Vicente-Serrano, S. M. and J.I. Lopez-Moreno. (2013). Streamflow droughts in the Iberian Peninsula between 1945 and 2005: spatial and temporal patterns, *Hydrol. Earth Syst. Sci.*, 17, 119-134.

Losleben, M., Burak, S., Davis, B., K. Adami. (2001). Snowfall occurrence at two lee-side mountain locations: comparing the Sierra Nevada, California and Rocky Mountains, Colorado. in: *Proceedings of the 18th Annual Pacific Climate Workshop*, edited by G. James West and Lauren Buffalo, Technical Report 69 of the Interagency Ecological Program for the San Francisco Estuary, pp 39-46, March 2002.

Lundquist, J.D., Minder, J. R., Neiman, P. J., Sukovich, E. (2010). Relationships between Barrier Jet Heights, Orographic Precipitation Gradients, and Streamflow in the Northern Sierra Nevada: *J. Hydrometeorology*, 11 (5), 1141-1156.

Mahood, G.A., Ring, J.H. Manganelli, S., McWilliams, M. O. (2010). New $^{40}\text{Ar}/^{39}\text{Ar}$ ages reveal contemporaneous mafic and silicic eruptions during the past 160,000 years at Mammoth Mountain and Long Valley caldera, California. *GSA Bulletin*: March/April 2010; v. 122; no. 3/4.

Mammoth Community Water District Groundwater Management Plan. (2005), retrieved from <http://www.mcwd.dst.ca.us/groundwater.html>.

Mammoth Community Water District Final Environmental Report.(2010). Retrieved from <http://www.mcwd.dst.ca.us/surface-water.html>.

McEvoy, D.J., J.L. Huntington, J.T. Abatzoglou and L.M Edwards. (2012). An Evaluation of Multiscaler Drought Indices in Nevada and Eastern California, *Earth Interactions*, V. 16 #18.

McEvoy, D.J., J.L. Huntington, J.T. Abatzoglou. (2013). A Comparison of the Standardized Precipitation Evapotranspiration Index Using the Penman-Monteith and Thornthwaite Parameterizations of Potential Evapotranspiration, *AMS Confex* 2013.

McKee, T. B., N. J. Doesken, and J. Kleist. (1993). The relationship of drought frequency and duration to time scales, *Proceedings Eight Conference on Applied Climatology*, Boston, MA, American Meteorological Society., 179-184.

Miller, J. A. *Groundwater Atlas of the United States*. (1999). *Hydrogeology Journal*, retrieved from <http://pubs.usgs.gov/ha/ha730/gwa.html>.

Mono County Upper Owens River Watershed Assessment (2007). Mono County Community Development Department, 2007.

Nippgen, F., B.L., McGlynn, L.A., Marshall, and R.E. Emanuel. (2011). Landscape structure and climate influences on hydrologic response, *Water Resources Research*, 47, W12528.

Peterson, D.H., I. Stewart, and F. Murphy. (2008). Principal Hydrologic Responses to Climatic and Geologic Variability in the Sierra Nevada, California, in San Francisco Estuary and Watershed Science, Vol 6, #1.

Peterson, D., Smith, R., Stewart, I. Knowles, N., Soulard, C. and S. Hager (2003). Snowmelt Discharge Characteristics Sierra Nevada, California. USGS SIR – 2005-5056.

Pierce, D.W., Barnett, T.P., Hildago, H.G., Tapash, D., Bonfils, C., Santer, B., Bala, G., Dettinger, M.D., Cayan, D.R., Mirin, A., Wood, A.W. and T. Nozawa (2008). Attribution of Declining Western U.S. Snowpack to Human Effects, Journal of Climate, Vol 21, 6425-6444.

Plummer, L. N., Prestemon, E. C. and D.L. Parkhurst. (1994). An Interactive Code (NETPATH) For Modeling NET Geochemical Reactions Along a Flow Path, U.S. Geological Survey Water Resources Investigation Report 94-4169.

Prudic, D. E., R.G. Niswonger and R. W. Plume. (2013). Trends in Streamflow on the Humboldt River between Elko and Imlay, Nevada, 1950-99, USGS Scientific Investigations Report 2005-5199.

Reid, J.B., Reynolds, J. L., Connolly, N.T., Getz, S.L., Polissar, P.J., and L.J. Windship. (1998). Carbon Isotopes in aquatic plants, Long Valley Caldera, California as records of past hydrothermal and magmatic activity. Geophysical Research Letters, Vol. 25, No. 15, pp 2853-2856.

Russell, Israel (1984) [Reprinted from the 1889 publication], Quaternary History of the Mono Valley, California, Eighth Annual Report of the United States Geological Survey, 1889, pages 267–394, Lee Vining, California; Originally, Washington, D.C.: Artemisia Press; Originally, the United States Geological Survey

Singh, P. and V.P. Singh. (2001). Snow and glacier hydrology, Kluwer Academic Publ.

Soil Science Society of America. (2001). Glossary of soil science terms (Online). Available at <https://www.soils.org/publications/soils-glossary/>

Sorey, M.L., Evans, W.C., Kennedy, B.M. Farrar, C.D., Hainsworth, L.J., and Hausback, B. (1998). Carbon dioxide and helium emissions from a reservoir of magmatic gas beneath Mammoth Mountain, California. Journal of Geophysical Research, v. 103, no. B7.

Stephens, J.C. and J.G. Hering. (2002). Comparative characterization of volcanic ash soils exposed to decade-long elevated carbon dioxide concentrations at Mammoth Mountain, California, Chemical Geology 186, 301– 313.

Stewart, I.T., Cayan, D.R. and M.D. Dettinger (2005). Changes towards earlier streamflow timing across western North America, Journal of Climate, 18:1136-1155.

Suemnicht, G. A. (1987). Results of Deep Drilling in the Western Moat of Long Valley, CA, Proceedings, 12th Workshop on Geothermal Reservoir Engineering, Stanford University, Stanford, C, January 1987.

Tague, C., and G. E. Grant. (2004). A geological framework for interpreting the low-flow regimes of Cascade streams, Willamette River Basin, Oregon, *Water Resour. Res.*, 40, W04303, doi:10.1029/2003WR002629.

Tague, C., G. Grant, M. Farrell, J. Choate and A. Jefferson. (2008). Deep groundwater mediates streamflow response to climate warming in the Oregon Cascades. *Climatic Change* 86; 189-210.

TEAM Engineering and Management, Inc. (2007). Hydrologic Assessment, Dry Creek Area, Mono County, California.

Tetra Tech.(2011). Task G: Los Angeles Aqueduct System Climate Change Study Final Report to Los Angeles Department of Water and Power.

Tempel, R. and D. Sturmer. (2011). Geochemical Modeling of the Near-Surface Hydrothermal System Beneath the Southern Moat of Long Valley Caldera, California. *Search and Discovery Article #80179 (21011)*.

Tierney, T. (2011). *Geology of the Mono Basin. Mono Lake Committee Field Guide Series*. Lee Vining: Kutsavi Press.

Thornthwaite, C.W. (1948). An approach toward a rational approach to climate. *Geogr. Rev.*, 38, 55-94.

USDA, Forest Service, Inyo National Forest, Mammoth Ranger District. (1994). Dry Creek Well and Pipeline Project, Environmental Assessment.

USDA Natural Resource Conservation Service. Soil Survey. (1995). Inyo National Forest West Area California.

United States Geological Survey. (2010). USGS observation spring sites at the Hot Creek Fish Hatchery in Long Valley caldera, California. Retrieved February 10, 2014, from https://137.227.239.76/lvo/activity/monitoring/hydrology/fhall_main.php

Vicente-Serrano, S.M., S. Begueria and J.I. Lopez-Moreno. (2010). A Multiscaler Drought Index Sensitive to Global Warming: The Standardized Precipitation Evapotranspiration Index, *Journal of Climate*, Vol. 23.

Vincente-Serrano, S.M. and J.I. Lopez-Moreno. (2005). Hydrological response to different time scales of climatological drought: an evaluation of the Standardized Precipitation Index in a mountainous Mediterranean basin. *Hydrology and Earth System Sciences*, 9.

Vincente-Serrano, S.M.; Begueria, S., Lorenzo-Lacruz, J.; Camerero, J.J.; Lopez-Moreno, J.I.; Azorin-Molina, C.; Revuelto, J.; Moran-Tejeda, E.; Sanchez-Lorenzo. (2012). A. Performance of Drought Indices for Ecological, and Hydrological Applications, *Earth Interactions*, vol. 16, issue 10.

Waring, G. A. (1915). *Springs of California*, U.S. Geological Survey Water-Supply Paper 338, 310 p.

Wildermuth, M.J. (1996). *Hydrologic Impacts of the Snowcreek Golf Course Expansion of the AB CD Headwater Springs*. Report prepared for Mammoth Community Water District.

Wildermuth Environmental, Inc. (2003). *Investigation of Groundwater Production Impacts On Surface Water Discharge and Spring Flow*, Final Report, Task Order Number 3, prepared for Mammoth Community Water District, 40 pp.

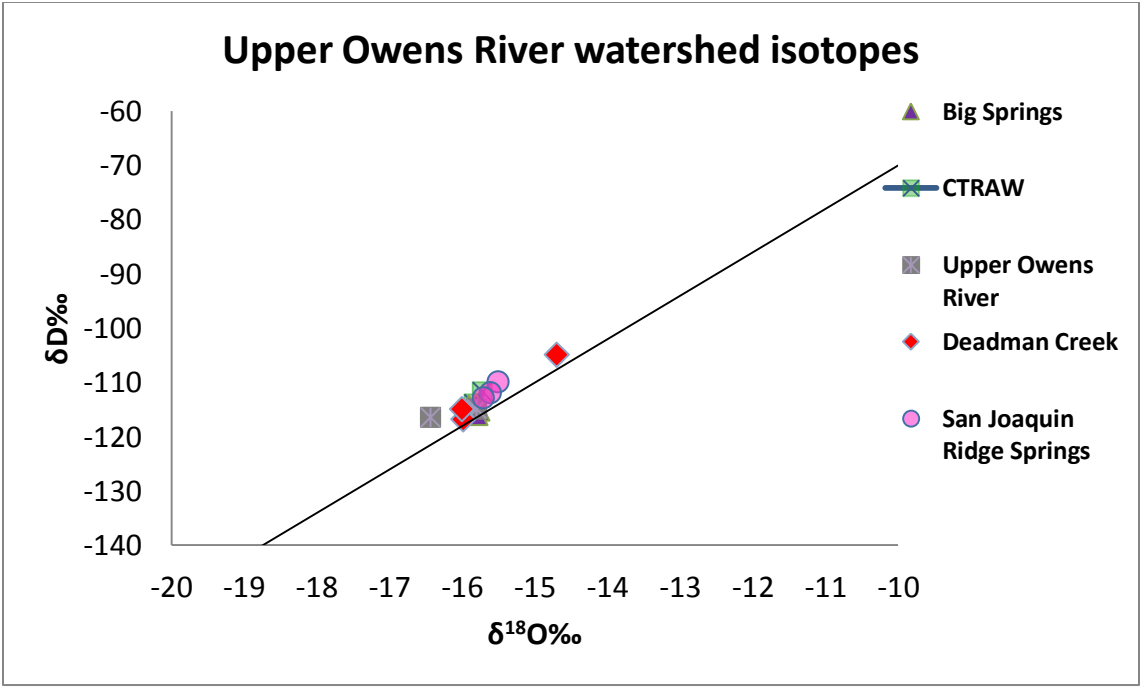
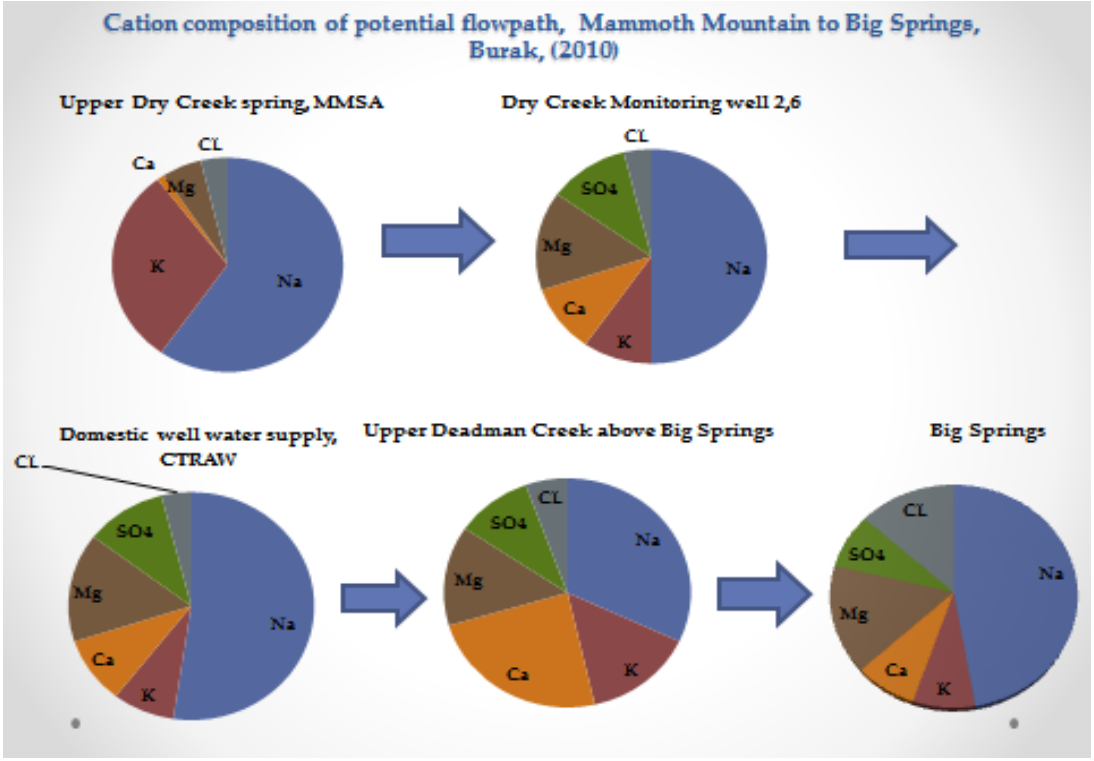
Wildermuth, M.J. (2009). *Mammoth Basin Groundwater Model Report*. Final Report. Prepared for the Mammoth Community Water District.

Wolf, J. W. (2012). *Evaluation of Drought Metrics in Tracking Streamflow in Idaho*, Ms. Thesis, University of Idaho.

Appendix A: Water chemistry Upper Owens River watershed

Major ion chemistry, surface and spring water

Location	Date	Bicarbonate alkalinity as CaCO ₃ -	HCO ₃ ⁻	pH	Cl-	NO ₃ ⁻	SO ₄ ⁻	Ca ²⁺	K+	Mg ²⁺	Na+	SiO ₂
Deadman Cr above BS	05/15/2009	25	30.5	7.1	0.81	< 0.25	0.88	3.58	1.99	2.05	4.4	17.3
Deadman Cr above BS	07/16/2009	23	28.1	7.0	0.63	< 0.25	1.69	2.71	1.72	1.65	4.07	15.6
Owens River below BS	07/16/2009	96.4	117.6	7.0	9.53	0.93	7.31	6.19	5.3	7.89	28.8	25.7
Owens River below BS	11/18/2009	103	125.7	7.1	9.15	0.53	6.21	7.49	5.44	8.82	30.2	26.7
Owens River below BS	10/10/2010	102	124.8	7.2	8.33	0.76	5.65	7.73	4.74	8.19	27.5	25.1
Big Springs PVC	07/13/2008	121	147.6	7.1	6.1	ND	6.1	9.3	6	12	36	24.8
Big Springs PVC	05/15/2009	125.1	147.6	7.0	7.64	0.9	7.88	6.81	6.15	9.49	34.4	28.8
Big Springs PVC	11/18/2009	121.9	150.2	7.1	7.04	0.68	6.33	7.7	5.85	10	33.3	28.1
Big Springs PVC	05/30/2010	132	161	7.1	7.2	0.9	6.51	7.15	4.89	10	29.2	27.2
Big Springs PVC	10/10/2010	104.9	128	7.1	10.9	0.58	6.34	5.23	4.45	6.41	24.7	21.8
Big Springs Nettle spr	07/13/2008	120	146.4	7.1	10	ND	5.3	7.6	4.9	7.9	28	ND
Big Springs Nettle spr	07/14/2009	149	182	7.0	8.01	0.53	7.48	6.62	5.87	8.92	32.4	27.7
Big Springs Nettle spr	05/30/2010	110	135.2	7.0	7.39	0.417	6.42	6.81	5.11	9.72	27.9	26.7
San Joaquin Ridge spr												
Spring 1	10/30/2008	15.4	18.3	7.1	<0.1	ND	0.21	1.8	2.6	1.1	1.8	ND
Spring 1	07/09/2009	9	11	6.8	0.22	0.71	0.34	1.02	1.75	0.77	1.25	16.8
Spring 12	10/30/2008	5.4	6.7	6.8	0.56	ND	2.23	0.56	1.73	0.59	1.08	12
Spring 12	07/09/2009	4.4	5.4	6.7	0.48	ND	2.15	0.63	1.53	0.63	1.12	5.7
Spring 3	06/25/2008	15	18.3	7.3	0.21	0.15	0.2	1.8	2.6	1.1	1.8	16
Spring 3	10/30/2008	12.6	15.5	7.0	0.17	ND	0.52	1.24	2.61	1	1.52	18.9



Appendix A: Water chemistry discussion

Dissolved chemistry of water discharging at Big Springs is distinguished from spring waters on the San Joaquin Ridge by high levels of Na^+ . Major ion concentrations of Deadman Creek and the San Joaquin Ridge springs are dilute and generally less than 10 mg/l. High elevation springs along San Joaquin Ridge represent a localized recharge area; spring water chemistry are Mg- SO_4 water type, reflecting the mineral content of quartzite, hornfels, amphiboles and olivine (Bailey 1989; Hildreth 2004; Hildreth et al. 2014). Spring waters have high K^+/Na^+ ratios (1.0-1.7) and $\text{Mg}^{+2}/\text{Na}^+$ (~0.6), typical of the earliest stage of rock weathering (Hem, 1985, Drever 2002, Evans et al. 2002). The SiO_2 concentrations are much higher than expected for Sierra cold springs, showing the influence of magmatic CO_2 gas on the dissolution of SiO_2 (Evans et al. 2001, Evans et al. 2002).

Spring waters on the San Joaquin Ridge have very low amounts of chlorine (Cl) ranging from less than detection levels of 0.1 mg/l to 0.81 mg/l in snowmelt-recharged springs. Slightly higher levels of chlorine are found in Deadman Creek. Extremely low concentrations of chlorine suggest very young waters that took rapid shallow flowpaths from recharge to discharge (Drever, 2002). Chlorine concentrations are ten times higher in Big Springs and the upper Owens River; 6 to 10 mg/l.

Cation chemistry shows the proportions of major cations derived from silicate weathering are similar along a flowpath between Mammoth Mountain to Big Springs. NETPATH (Plummer et al. 1994) modeling showed SiO_2 precipitating along a hypothetical flowpath from upper Dry Creek spring to Big Springs, which is expected for weathering of silicates (Evans et al. 2001, Burak, 2010).

Isotopic signatures cluster along the global meteoric water line, indicating meteoric sources of water for the San Joaquin Ridge springs, Deadman Creek, and the upper Owens River downstream of Big Springs. Big Springs isotopic composition resembles surface water and plots close to the global meteoric water line indicating recharge of meteoric water with little or no evapotranspiration (Clark and Fritz, 1997). One sample of Deadman Creek water collected in mid-July plots to the right of the GMWL, indicating evaporation has occurred (Clark and Fritz, 1997). According to the water chemistry and hydrogeologic framework of the basins, the conceptual model of groundwater recharge and subsurface flow groundwater flow is consistent with the water chemistry and SPEI results.

Appendix B. SPEI Formulation

The SPEI uses the monthly difference between precipitation and PET. This represents a simple climatic water balance, which is calculated at different time scales to obtain the SPEI. In this study, the Thornthwaite equation (Thornthwaite, 1948) was used to estimate monthly PET in cm/month.

$$PET = 1.6 \left(\frac{L}{12} \right) \left(\frac{N}{30} \right) \left(\frac{10 T_a}{I} \right)^\alpha$$

T_a is the average daily temperature (degrees Celsius; if this is negative, use 0) of the month being calculated. If T_a is negative, PET is 0.

N is the number of days in the month being calculated.

L is the average day length (hours) of the month being calculated

$$\alpha = (6.75 \times 10^{-7})I^3 - (7.71 \times 10^{-5})I^2 + (1.792 \times 10^{-2})I + 0.49239$$

I is a heat index which depends on the 12 monthly mean temperatures T_{ai} .

$$I = \sum_{i=1}^{12} \left(\frac{T_{ai}}{5} \right)^{1.514}$$

Climatic water balance, P-PET (precipitation minus evapotranspiration)

Once PET is calculated from the Thornthwaite equation, the difference between the precipitation P and PET for the month i is calculated.

$$D_i = P_i - PET_i$$

P-PET values are either positive, indicating water surplus, or negative, indicating water deficits for each analyzed month. For this study, D_i values are aggregated at the 12, 15, 24, 36 and 48-month time scales.

Standardization of the variable

The log-logistic distribution shows a gradual decrease in the curve for low values of D , corresponding to 1 occurrence in 200 to 500 years. No values occur at the origin parameter of the distribution (Vicente-Serrano et al. 2010).

The probability density function of a three parameter log-logistic distributed variable is expressed as:

$$f(x) = \frac{\beta}{\alpha} \left(\frac{x - \gamma}{\alpha} \right)^{\beta-1} \left(1 + \left(\frac{x - \gamma}{\alpha} \right)^{\beta} \right)^{-2}$$

where α , β and γ are scale, shape and origin parameters, respectively, for D values in the range ($\gamma > D < \infty$). Parameters of the log-logistic distribution are obtained using the L-moment procedure (Ahmad et al., 1988).

$$\beta = \frac{2W_1 - W_0}{6W_1 - W_0 - 6W_2}$$

$$\alpha = \frac{(W_0 - 2W_1)\beta}{\Gamma(1 + \frac{1}{\beta})\Gamma(1 - \frac{1}{\beta})}$$

$$\gamma = W_0 - \alpha\Gamma\left(1 + \frac{1}{\beta}\right)\Gamma\left(1 - \frac{1}{\beta}\right)$$

where $\Gamma(\beta)$ is the gamma function of β .

In Vicente-Serrano et al. (2010), the probability weighted moments (PWM's) method was used when the log-logistic α , β and γ distribution parameters were calculated. The PWM's were obtained using the unbiased estimator of Hosking (1986). The unbiased PWM's are obtained according to:

$$w_s = \frac{1}{N} \sum_{i=1}^N \frac{\binom{N-i}{s} D_i}{\binom{N-1}{s}}$$

where N is the number of data, F^i is a frequency estimator following the approach of Hosking (1990) and D_i is the difference between Precipitation and Potential Evapotranspiration for the month i .

The probability distribution function of D according to the log-logistic distribution is:

$$F(x) = \left[1 + \left(\frac{\alpha}{x - \gamma} \right)^\beta \right]^{-1}$$

With $F(x)$ the SPEI is obtained as the standardized values of $F(x)$:

$$SPEI = W - \frac{C_0 + C_1W + C_2W^2}{1 + d_1W + d_2W^2 + d_3W^3},$$

where

$$W = -2 \ln(P).$$

For $P \leq 0.5$, P is the probability of exceeding a determined D value, $P = 1 - F(x)$.

If $P > 0.5$, is replaced by $1 - P$ and the sign of the resultant SPEI is reversed. The

constants are: $C_0 = 2.515517$, $C_1 = 0.802853$, $C_2 = 0.010328$, $d_1 = 1.432788$,

$d_2 = 0.189269$, $d_3 = 0.001308$. The average value of the SPEI is 0, and the standard

deviation is 1. The SPEI is a standardized variable; an SPEI of 0 indicates a value

corresponding to 50% of the cumulative probability of D , according to a log-logistic

distribution.

Equations and text in the appendix are excerpted from
<http://sac.csic.es/spei/home.html>.

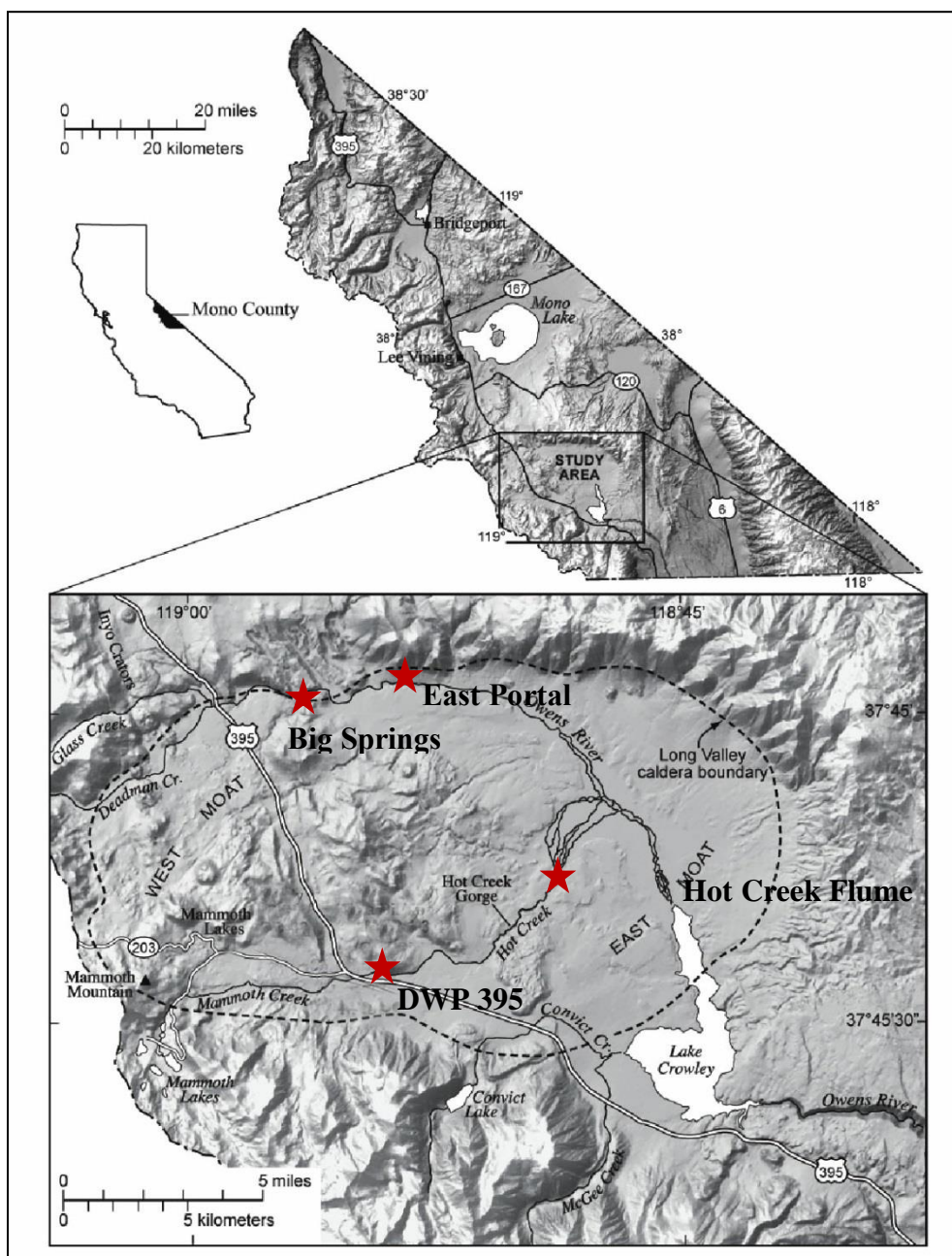


Figure 1. Location map of study area including the Long Valley caldera. Streamflow gage locations shown in red. Adapted from Tempel and Sturmer, 2011.

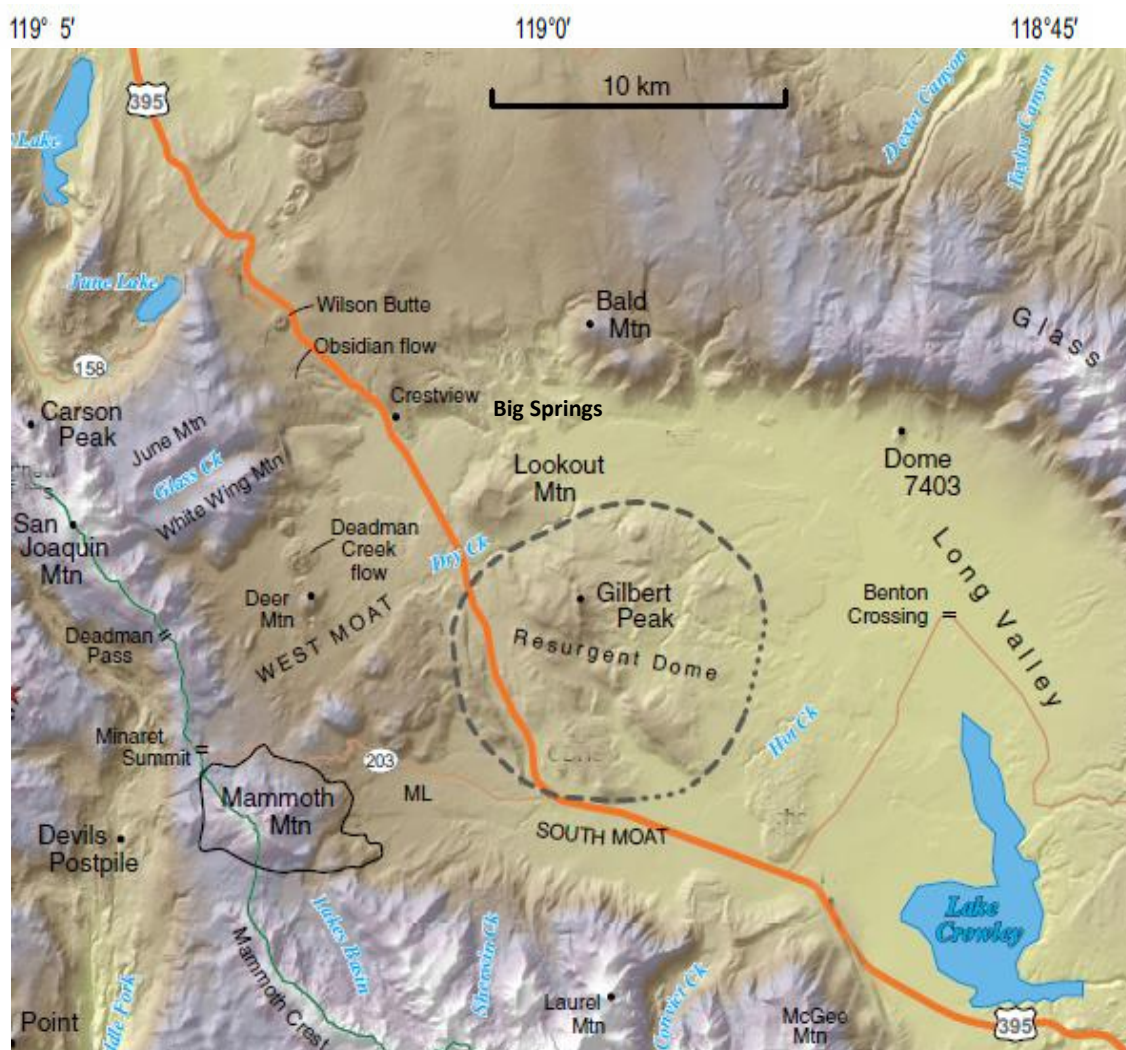


Figure 2. Shaded relief map centered on the Long Valley caldera. Mammoth Mountain is located at the southwest margin of the Long Valley caldera. The Mammoth Crest and San Joaquin Ridge (Minaret Summit to San Joaquin Mountain) form the drainage divide between the San Joaquin River and the Great Basin. Graphic adapted from Hildreth et al. 2014 with permission.

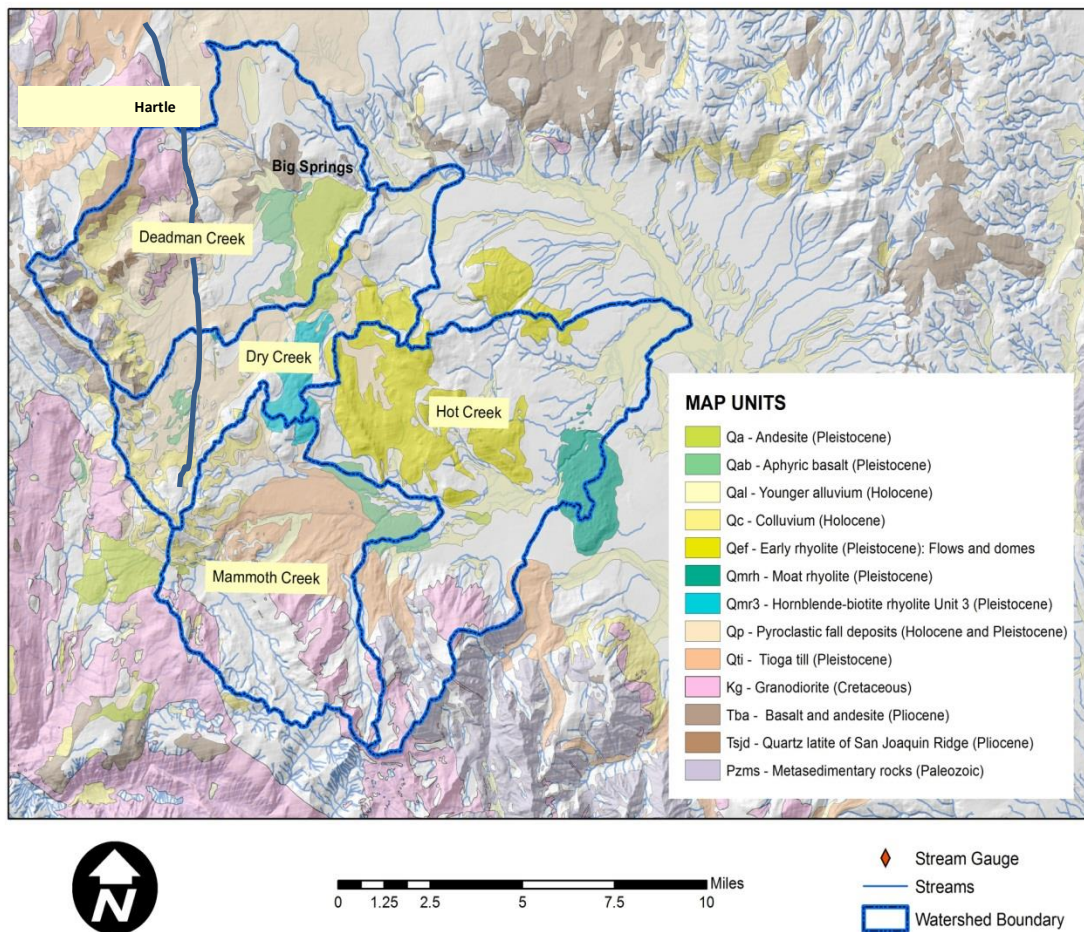


Figure 3. Geological map of the Long Valley caldera (adapted from Bailey, 1989).

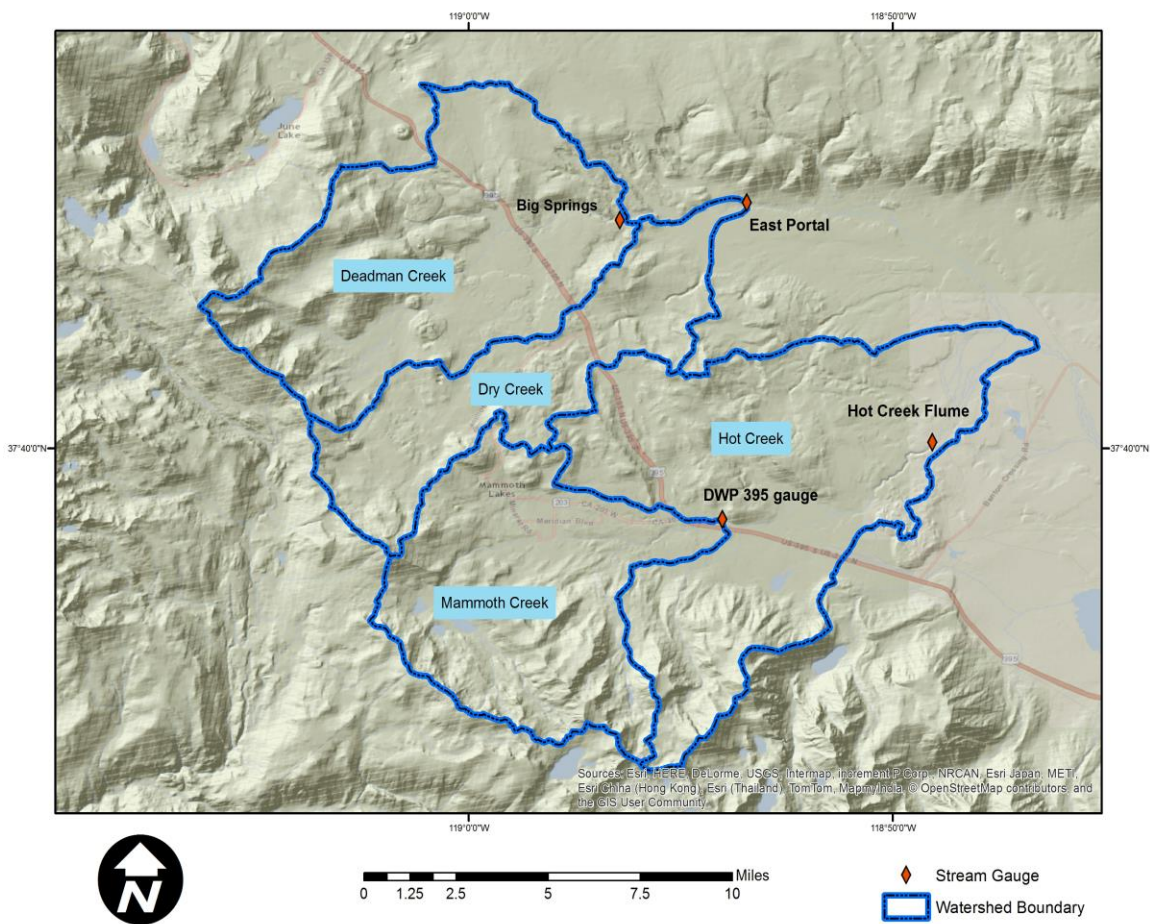


Figure 4. Watershed areas and streamflow gauges in the study area.

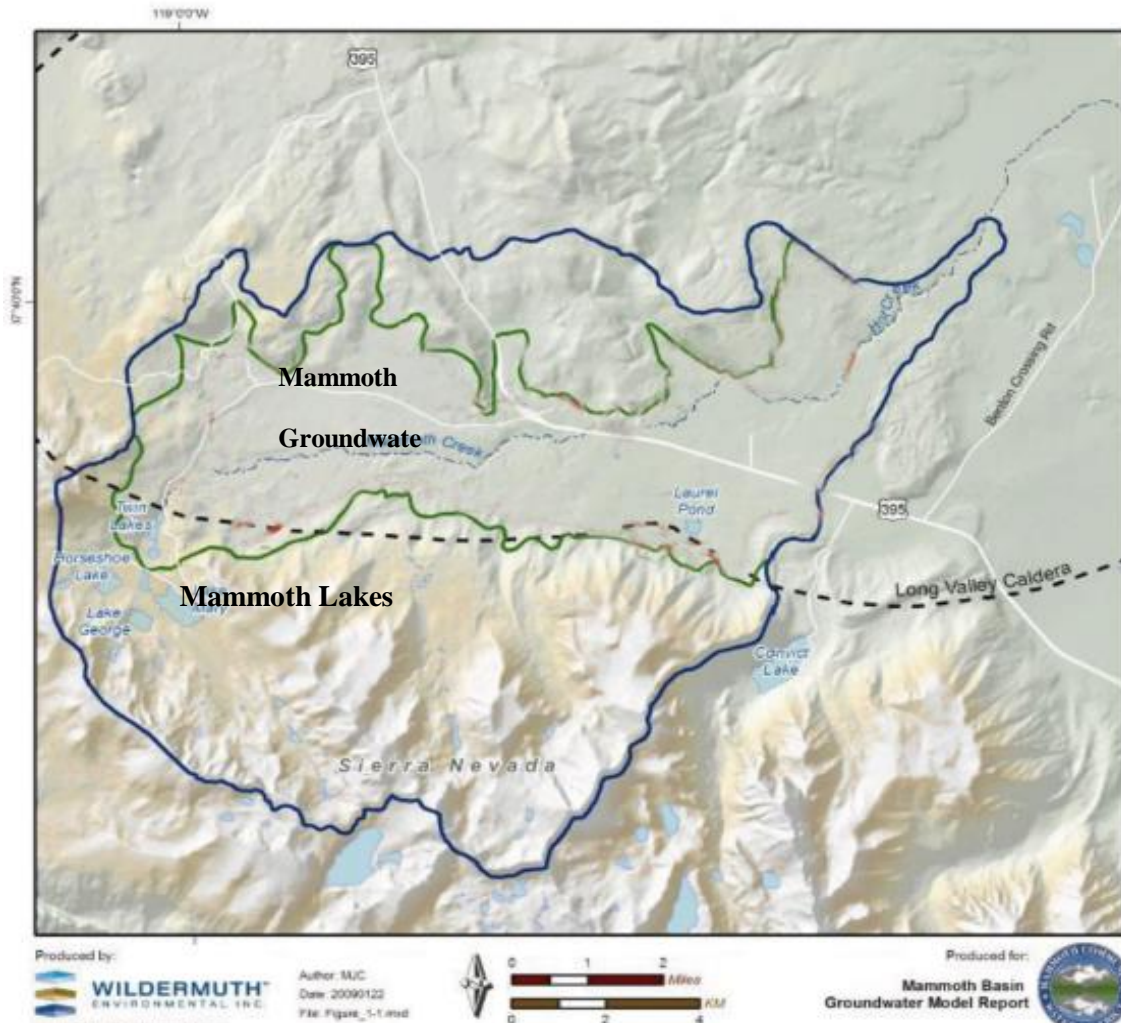


Figure 5. Mammoth Creek watershed. The Mammoth Groundwater Basin is outlined in green. Adapted from Wildermuth, 2009.

General characteristics of the study watersheds					
	Gage No.	Drainage Area (mi ²)	Datum of gage, ft..	Elev. range (ft..)	Annual pcp. (in)*
Upper Owens River	5052 (DWP)	71.9	7,104	7,104- 11,600	22.6
Mammoth Creek	10265130	33.8	7,213	7,200- 11,600	26.4
Hot Creek	10265150	68.3	6,950	6,950- 12,462	28.6

Table 1. General characteristics of the study watersheds

*PRISM precipitation

Precipitation station	Operator	Elevation ft..	Mean annual precipitation, inches	Period of record
Mammoth Pass	DWP	9,300	50.2	1928- present
Lake Mary precipitation gage	MCWD	8,900	29.1	1951-present
Mammoth Ranger Station	NWS coop	7,800	23.1	1981-present
SNARL Crowley Lake Dam	UCLA DWP	7,085 6,700	12.5 10	1948-present
Gem Lake	NWS coop	8,970	21.5	1924-2010

Table 2. Precipitation stations.

Data sources: <http://cdec.water.ca.gov>; Mammoth Community Water District;
<http://www.wrcc.dri.edu/cgi-bin/cliMAIN.pl?ca5280>;
 University of California Los Angeles, Sierra Nevada Research Laboratory (SNARL);
 Los Angeles Department of Water and Power;
<http://www.wrcc.dri.edu/cgi-bin/cliMAIN.pl?ca3369>

Basin name	Mean annual runoff, ac-ft. (1951-2011)	Median annual runoff, ac-ft.	WY Maximum discharge, ac-ft.	WY Minimum discharge, ac-ft	Coef. of variation
Upper Owens River	42,360	42,945	73,519 (1983)	25,508 (1992)	0.24
Mammoth Creek	16,472	15,356	45,813 (1983)	3,151 (1977)	1.4
Hot Creek	43,980	41,322	72,128 (1969)	25,437 (1961)	0.49

Table 3. Streamflow characteristics

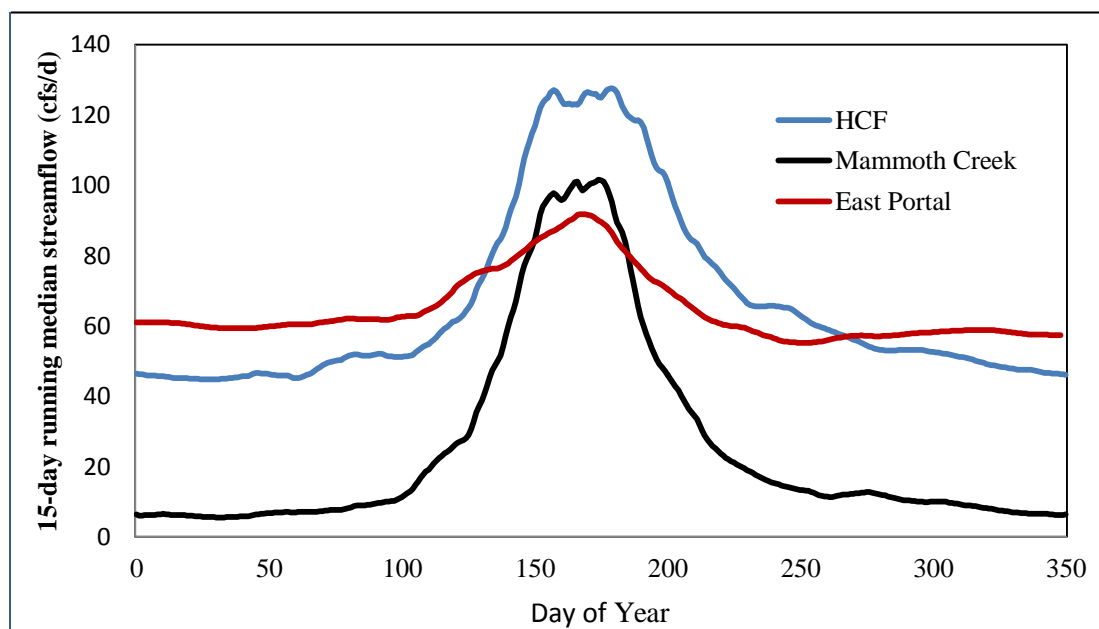


Figure 6. Snowmelt discharge hydrology; upper Owens River at East Portal, Mammoth Creek at DWP 395 and Hot Creek at Hot Creek Flume, water years 1951-2011. Mammoth Creek quickly returns to baseflow following peak flow; the upper Owens River and Hot Creek have higher base flows due to groundwater contributions.

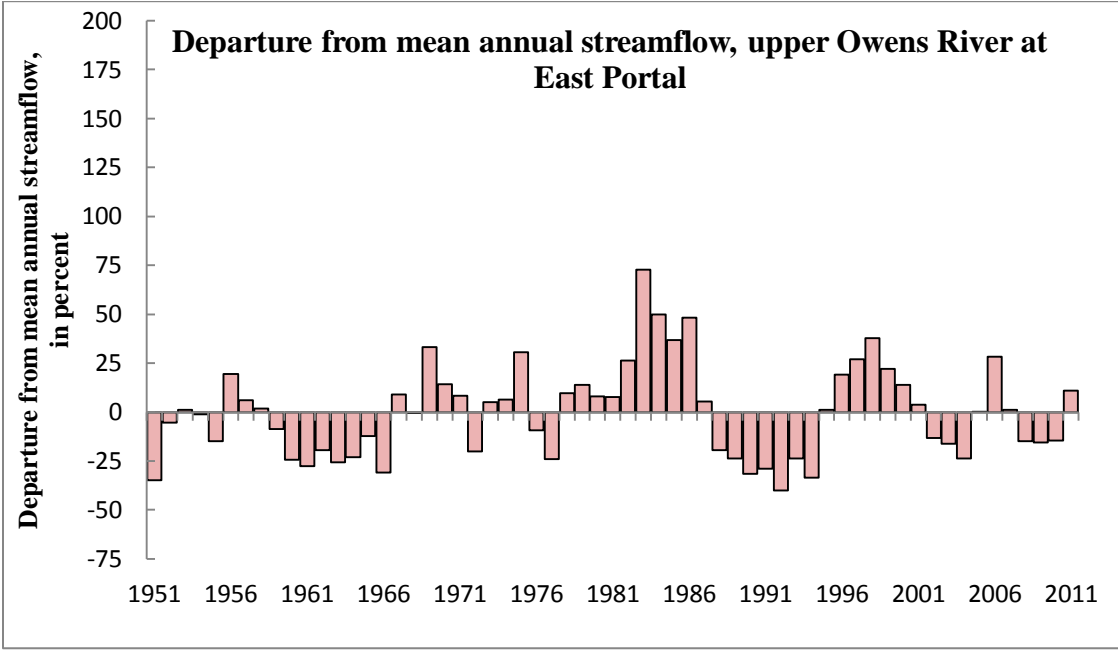


Figure 7. Departure from mean annual streamflow, upper Owens River at East Portal.

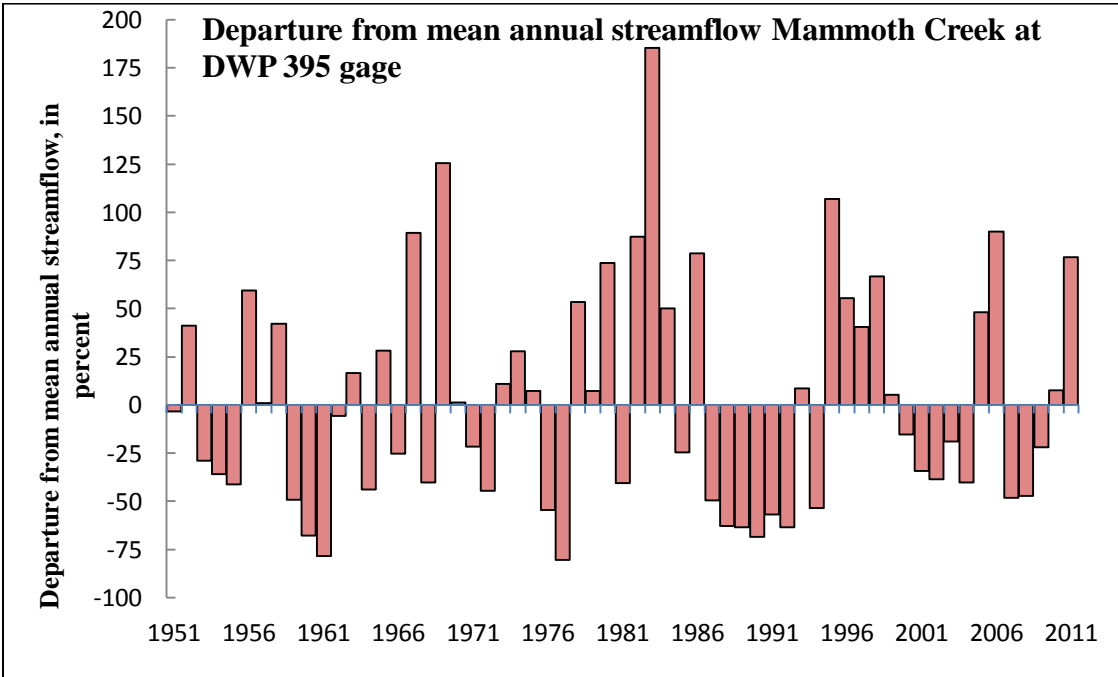


Figure 8. Departure from mean annual runoff, Mammoth Creek at DWP Old 395 gage.

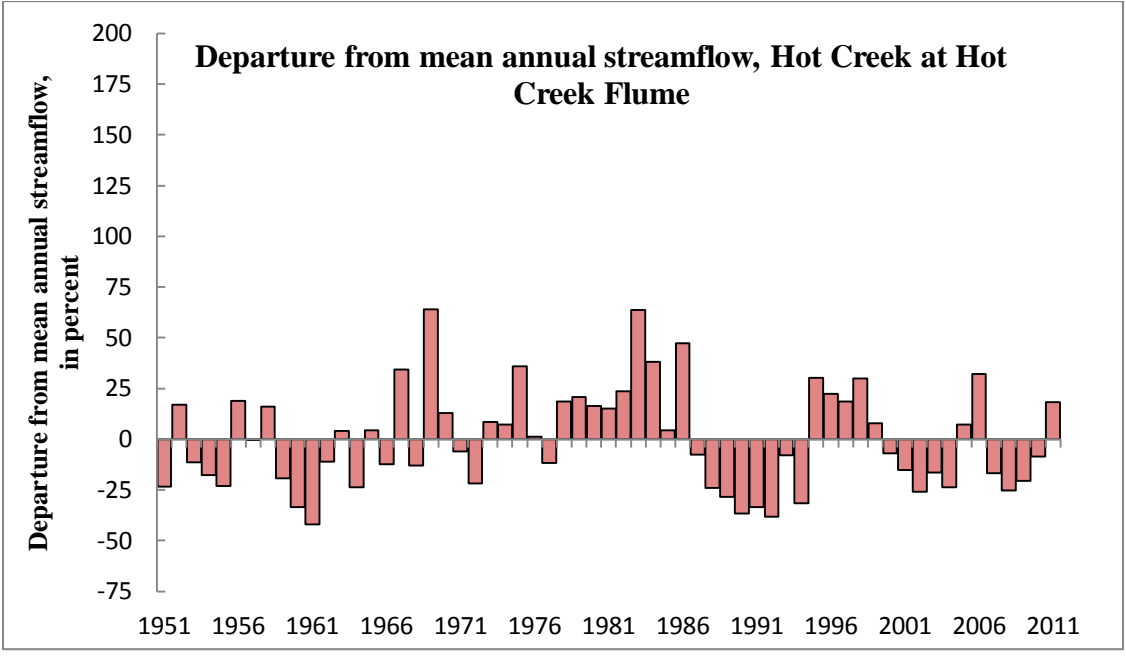


Figure 9. Departure from mean annual runoff, Hot Creek at the USGS Hot Creek Flume.

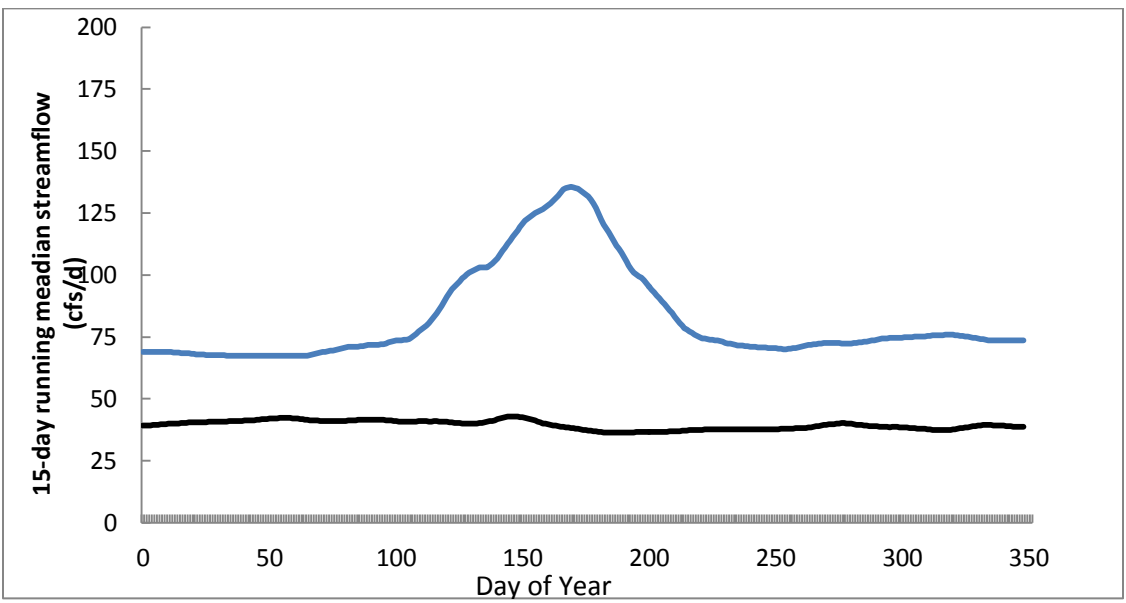


Figure 10. Average of the annual hydrograph for the wettest (black) and driest (grey) 5 years of record of upper Owens River flows measured at East Portal. Streamflow in the groundwater dominated upper Owens River watershed declines in dry years due to loss of Deadman Creek flows to the river above the Big Spring complex. Peak flows in wet years are muted due to groundwater contributions.

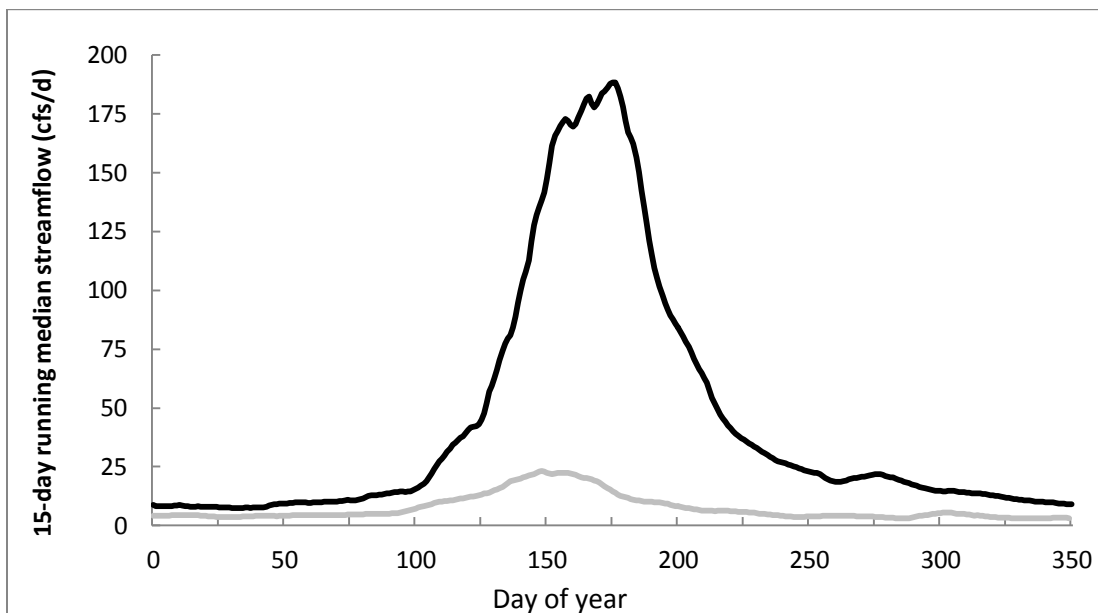


Figure 11. Average of the annual hydrograph for the wettest (black) and driest (grey) 5 years of record at Mammoth Creek measured at the DWP Old 395 gage. Low flows are lower and reach a minimum value earlier in dry years than in wet years. Peak flow occurs 15 to 25 days earlier in dry years relative to wet years.

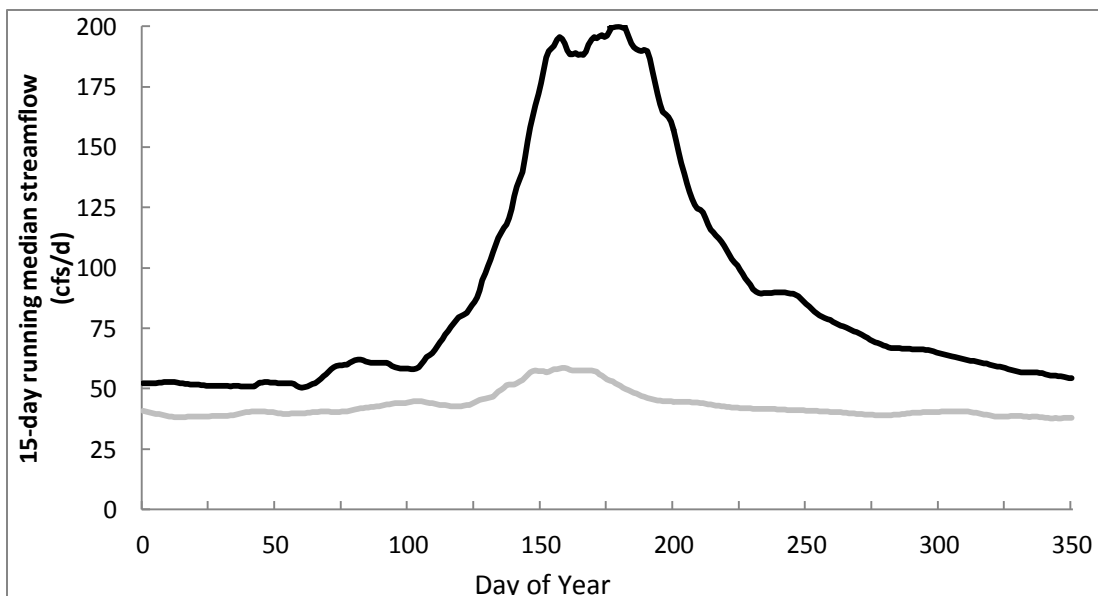


Figure 12. Average of the annual hydrograph for the wettest (black) and driest (grey) 5 years of record at the Hot Creek Flume. Peak flow occurs 20 to 30 days earlier in dry years than during wet years. The input of 20,000 to 25,000 acre-feet per year from the Hot Creek Fish Hatchery springs maintains consistent flows during dry years.

SPEI CLASS	Class Description
$SPEI \leq -2$	Extremely dry
$-2 < SPEI \leq -1.5$	Severely dry
$-1.5 < SPEI \leq -1$	Moderately dry
$-1 < SPEI \leq 0$	Mild drought
$0 < SPEI \leq 1$	Near normal wet
$1 < SPEI \leq 1.5$	Moderately wet
$1.5 < SPEI \leq 2$	Very wet
$SPEI > 2$	Extremely wet

Table 4. Explanation of SPEI categories, From Guttman, 1999.

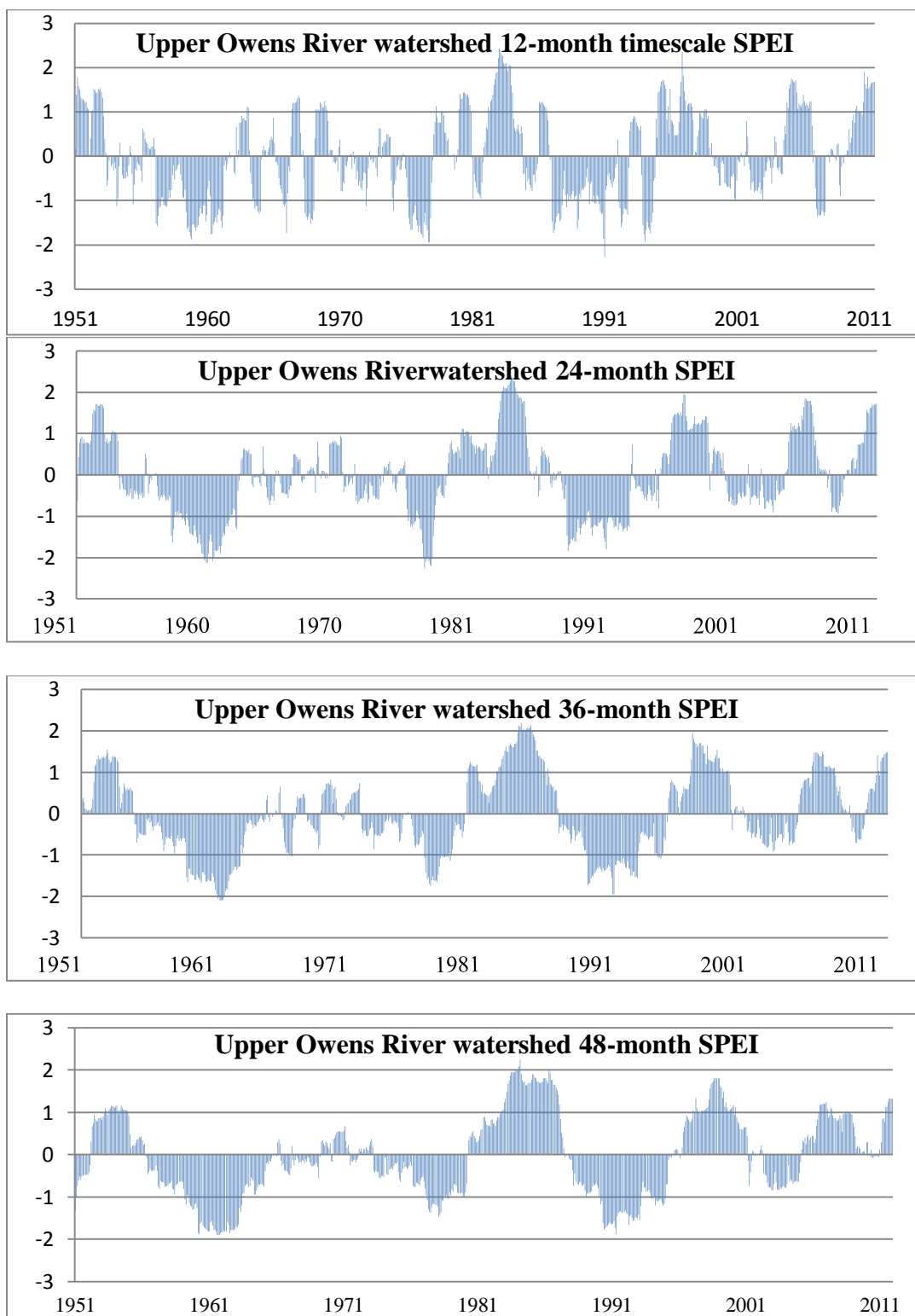


Figure 13. Historical time series of SPEI for the upper Owens River watershed at the 12, 24, 36 and 48-month time scales.

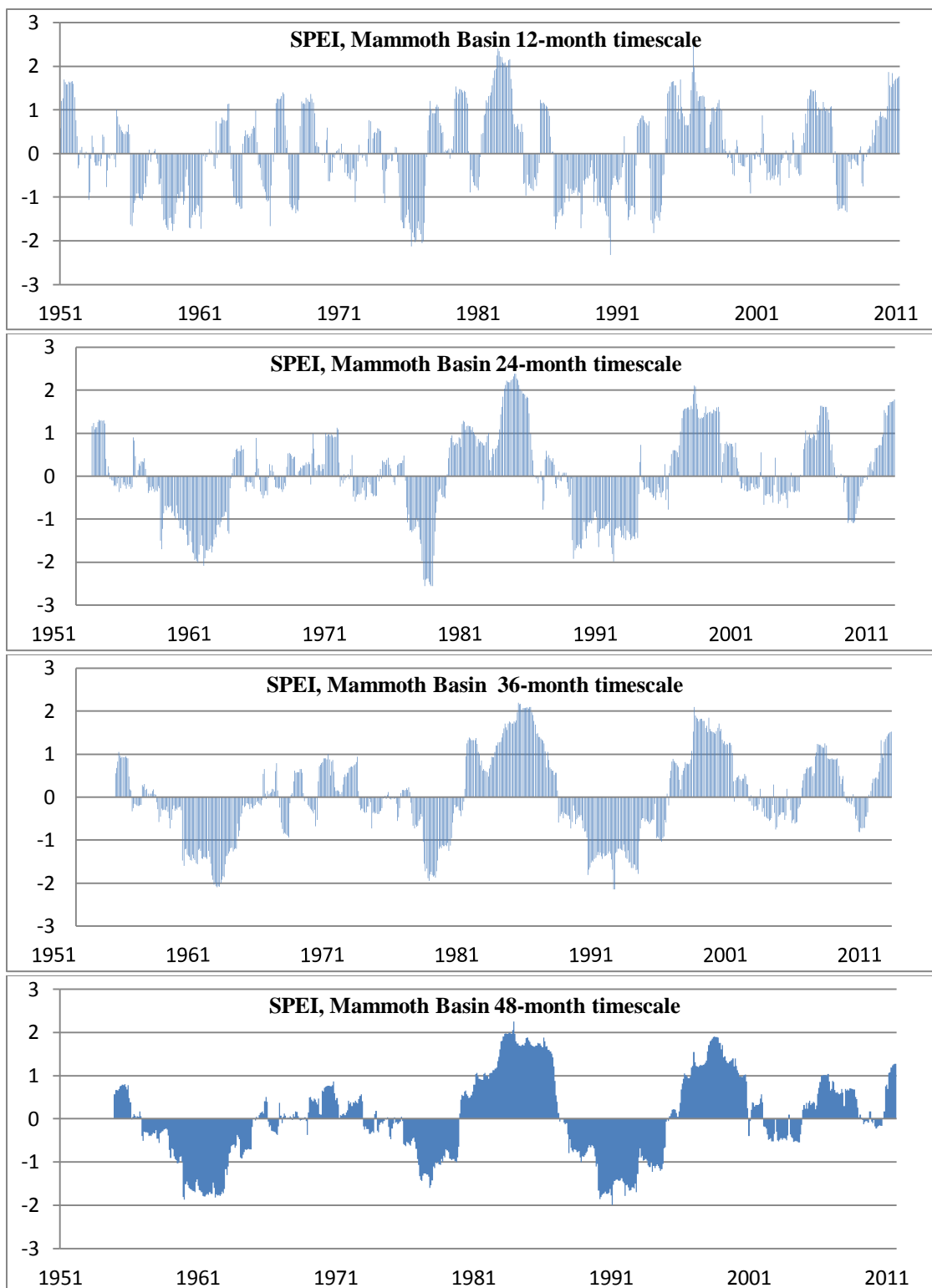


Figure 14. Historical time series of SPEI for the Mammoth Basin watershed at the 12, 24, 36 and 48-month time scales.

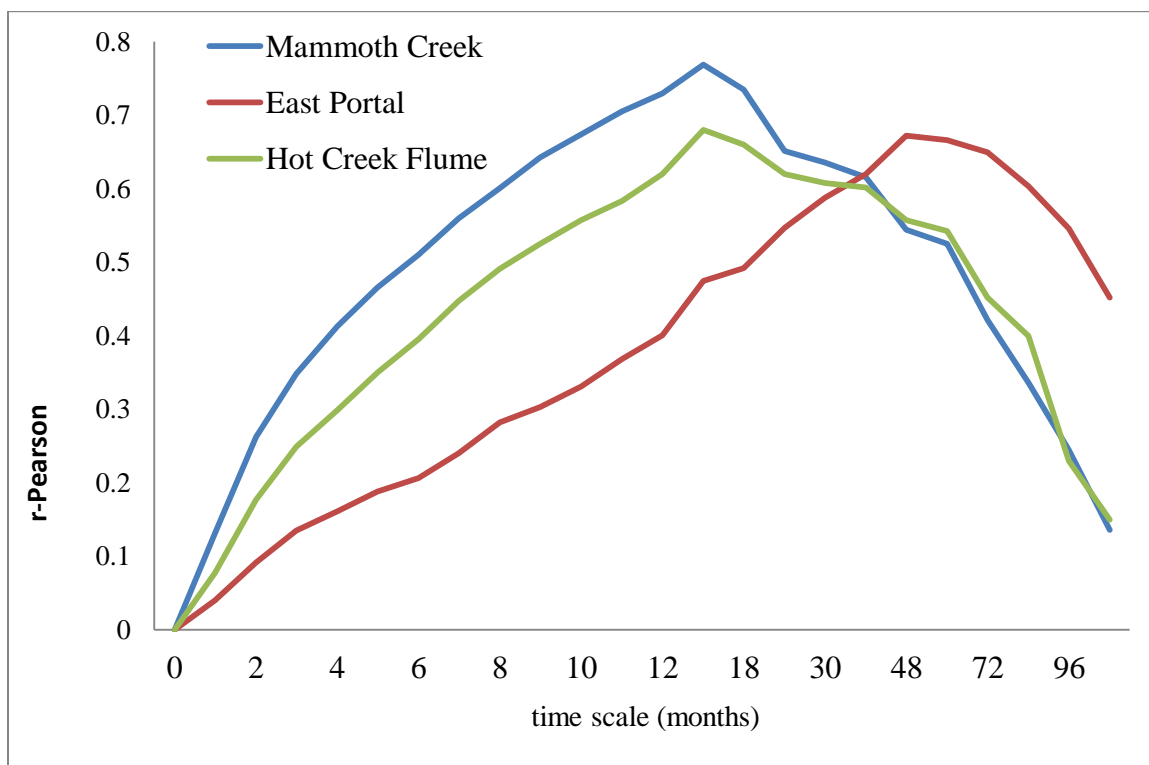


Figure 15. Continuous correlations between PRISM-based SPEI and standardized streamflow, Mammoth Creek, Hot Creek Flume and East Portal.

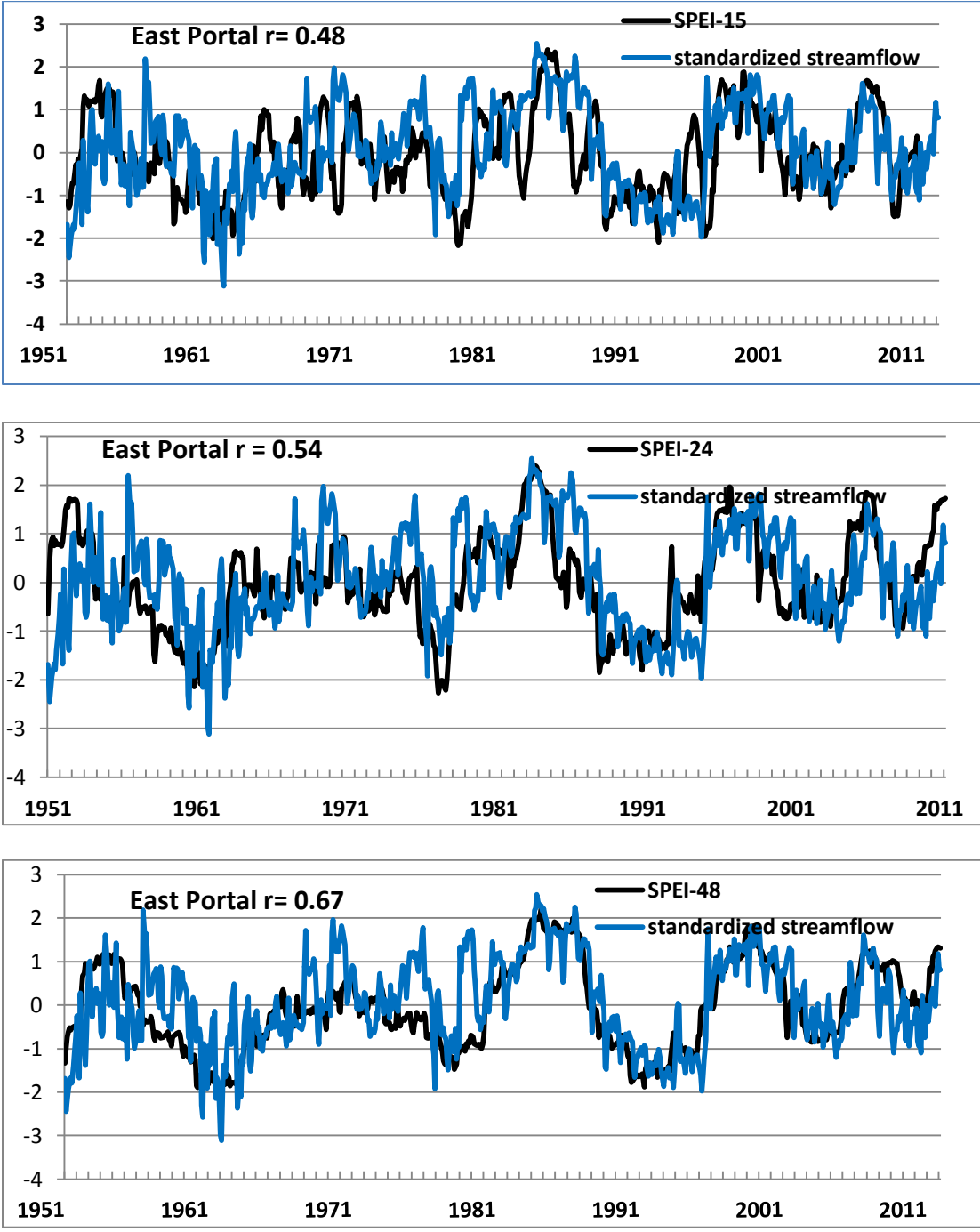


Figure 16. Temporal variability of the SPEI and standardized streamflow at the 15, 24 and 48- month scale, upper Owens River, East Portal. The Pearson correlation coefficient is used for comparison.

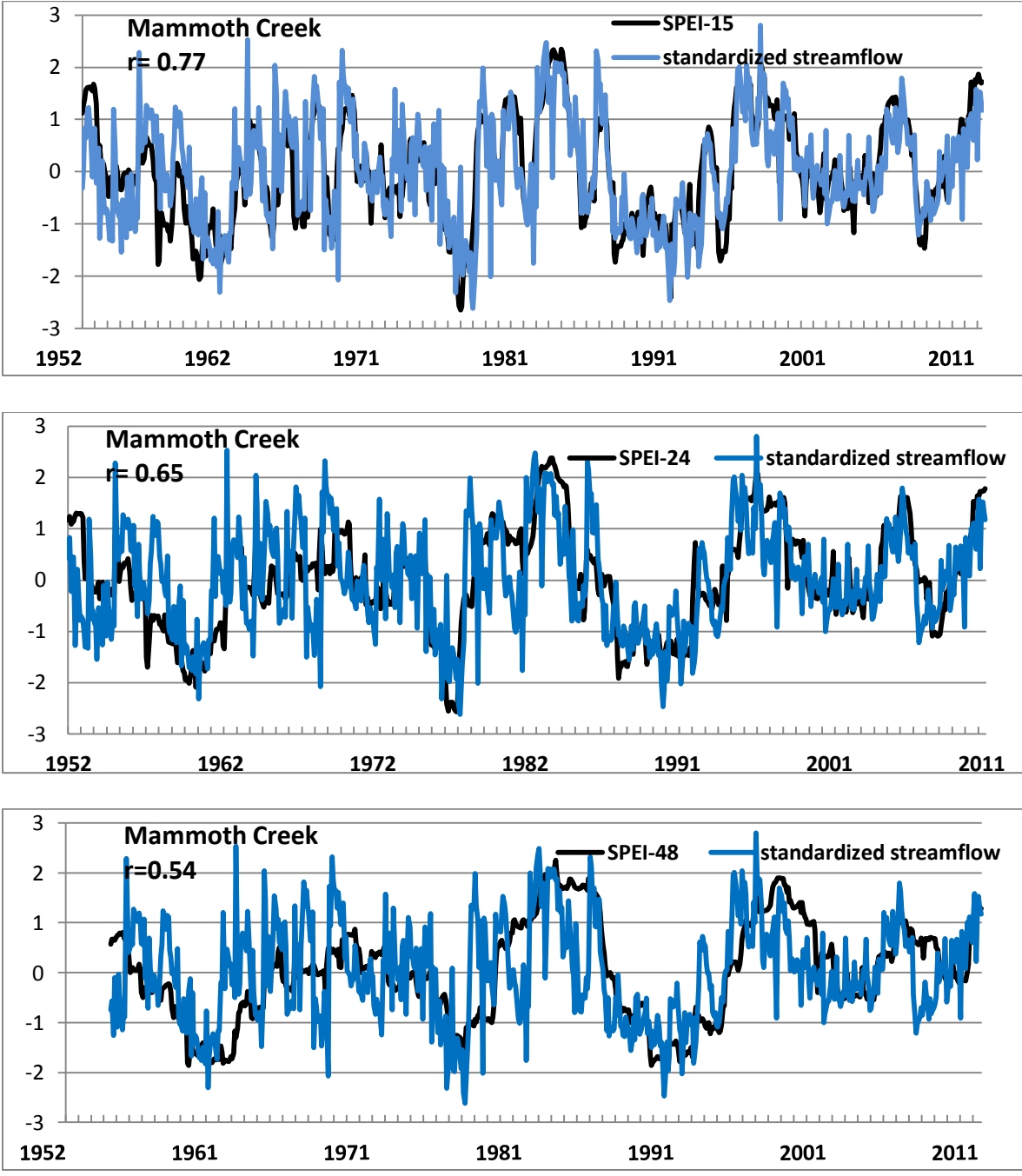


Figure 17. Temporal variability of the SPEI and standardized streamflow at the 15, 24, and 48-month time scale, Mammoth Creek at the DWP gage. The Pearson correlation coefficient is used for comparison.

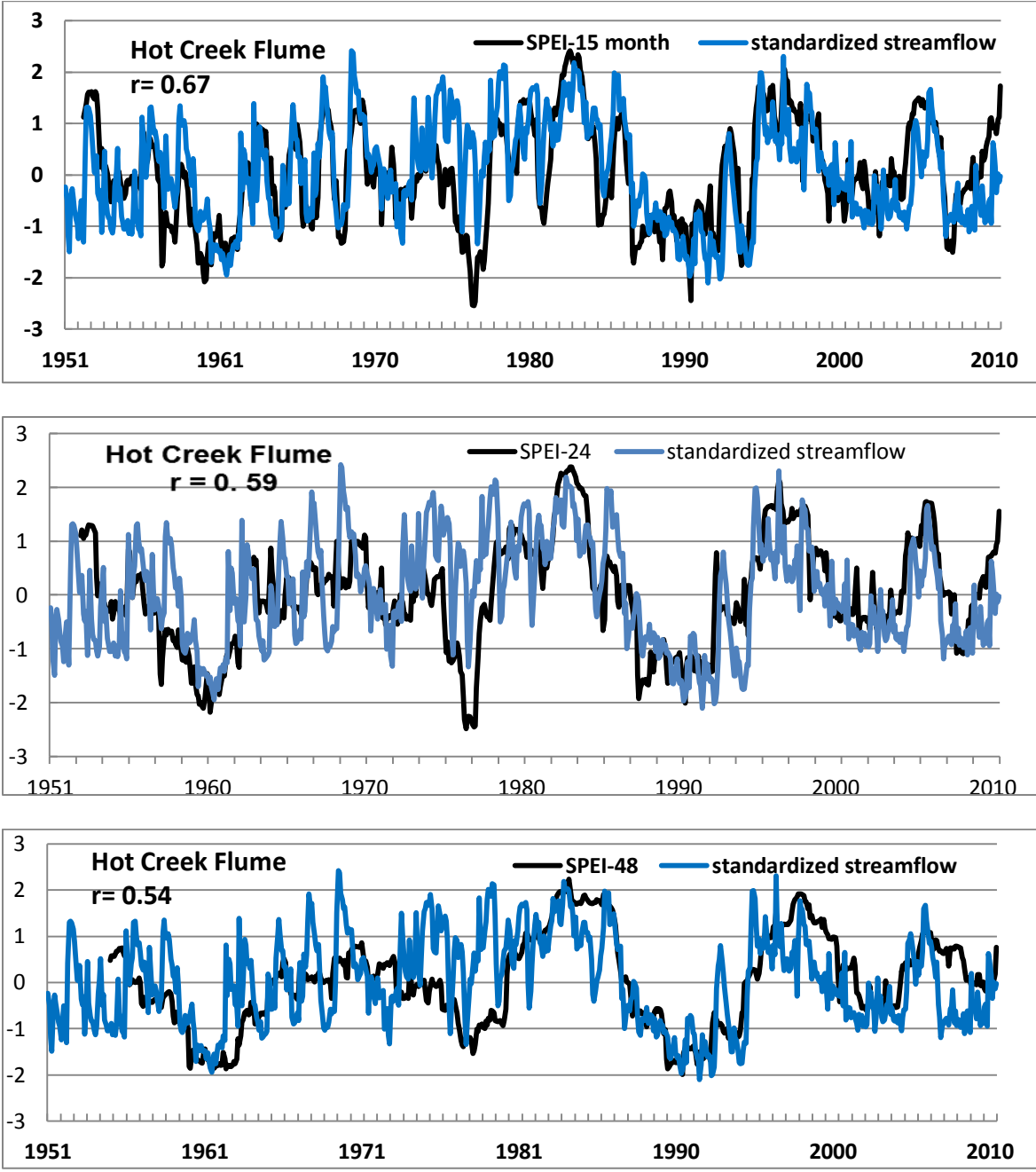


Figure 18. Temporal variability of the SPEI and standardized streamflow at the 15, 24, and 48-month time scale, Hot Creek at the Hot Creek Flume. The Pearson correlation coefficient is used for comparison.

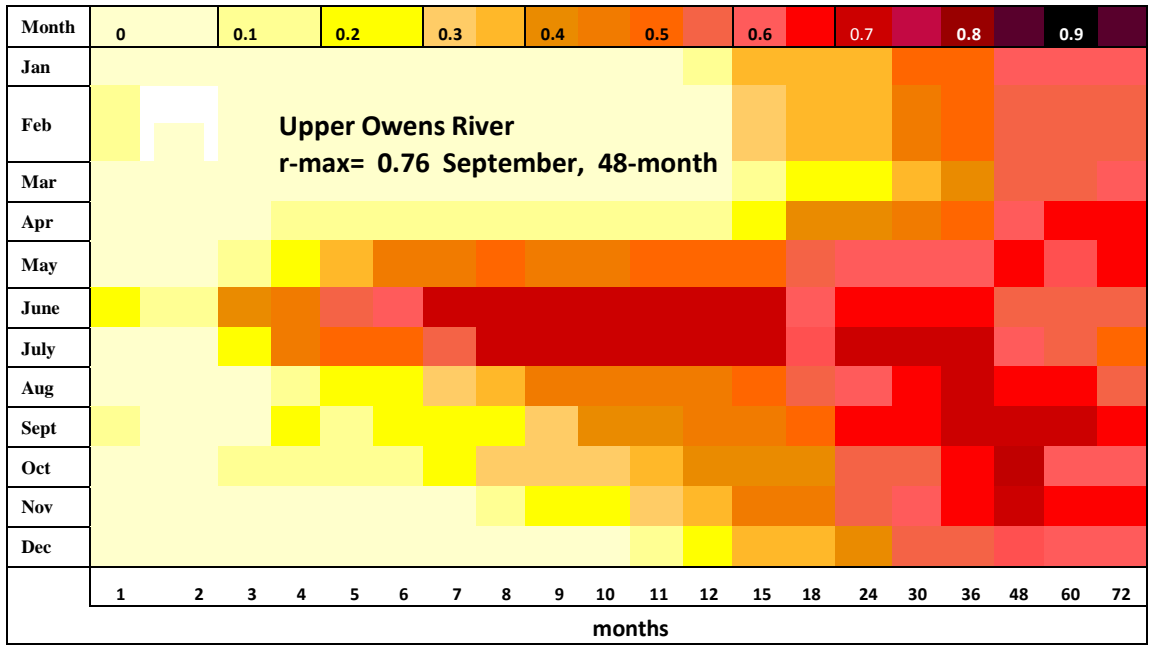


Figure 19. Monthly correlations between streamflow and SPEI, upper Owens River at East Portal. Streamflow and the SPEI are well correlated in June and July at the 8 to 15-month timescale and at longer timescales of 36 to 48-months. The highest correlations (0.76) occur in September and November at the 48-month time scale.

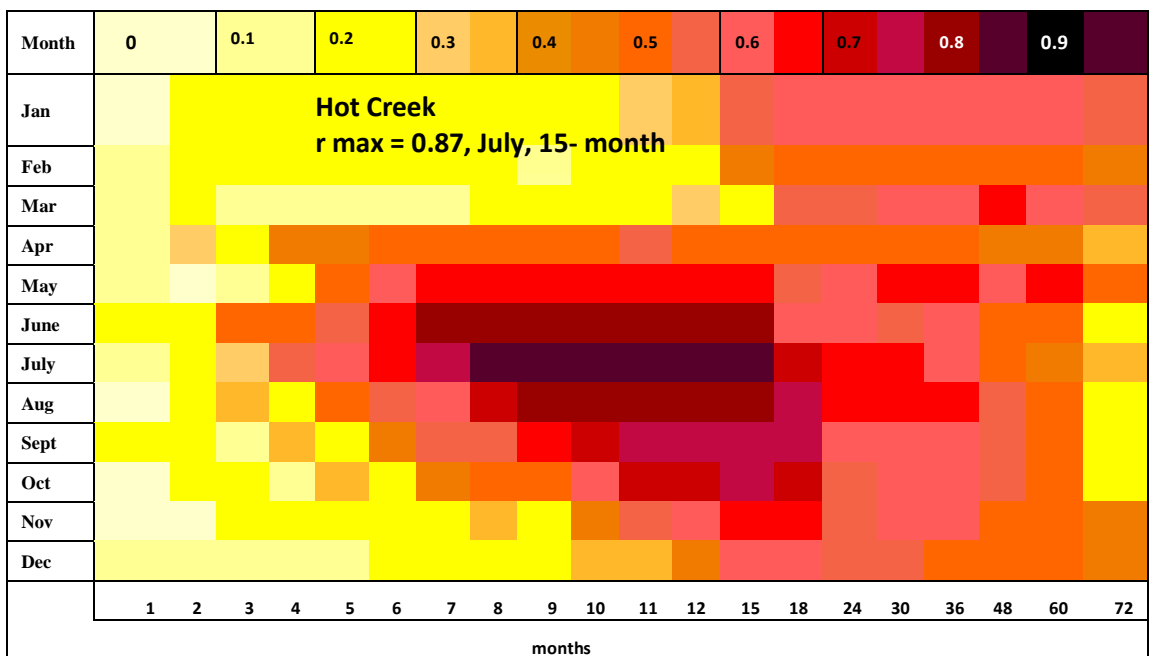


Figure 20. Monthly correlations between SPEI and standardized streamflow, Hot Creek at the Hot Creek Flume. Streamflow and SPEI are well correlated during June, July and

August at the 7 to 15-month timescale. Highest correlations (0.87) occur in July at the 8 to 15-month timescale.

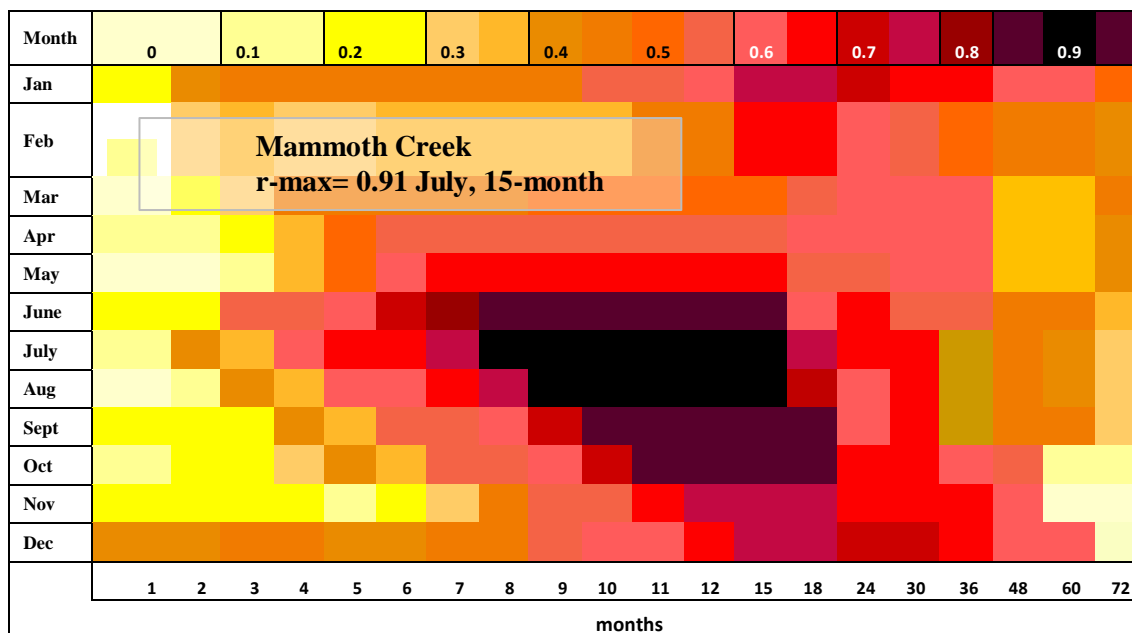


Figure 21. Monthly correlations between SPEI and standardized streamflow, Mammoth Creek at the DWP 395 gage. Streamflow and SPEI are highly correlated in July and August at the 8 to 15-month timescale. Highest correlations (0.91) occur in July and August.